

1 **A diverse host thrombospondin-type-1 repeat protein repertoire promotes symbiont**
2 **colonization during establishment of cnidarian-dinoflagellate symbiosis**

3

4 Authors: Emilie-Fleur Neubauer¹, Angela Z. Poole^{2,3}, Philipp Neubauer⁴, Olivier Detournay⁵,
5 Kenneth Tan³, Simon K. Davy^{1*} & Virginia M. Weis^{3*}

6 ¹School of Biological Sciences, Victoria University of Wellington, Wellington, New Zealand

7 ²Department of Biology, Western Oregon University, Monmouth, OR, USA

8 ³Department of Integrative Biology, Oregon State University, Corvallis, OR, USA

9 ⁴Dragonfly Data Science, Wellington, New Zealand

10 ⁵ Planktovie sas, 13190 Allauch, France

11

12

13 **Keywords:** TSR, thrombospondin, coral, symbiosis, *Symbiodinium*, innate immunity, *Aiptasia*
14 *pallida*

15

16 **Corresponding author:**

17 *Corresponding authors: simon.davy@vuw.ac.nz; Tel: +64-4-4635573, weisv@oregonstate.edu;
18 Tel: 1-541-737-4359

19

20

21 **Abstract**

22
23 The mutualistic endosymbiosis between cnidarians and dinoflagellates is mediated by complex
24 inter-partner signaling events, where the host cnidarian innate immune system plays a crucial
25 role in recognition and regulation of symbionts. To date, little is known about the diversity of
26 thrombospondin-type-1 repeat (TSR) domain proteins in basal metazoans and or their potential
27 role in regulation of cnidarian-dinoflagellate mutualisms. We reveal a large and diverse
28 repertoire of TSR proteins in seven anthozoan species, and show that in the model sea anemone
29 *Aiptasia pallida* the TSR domain promotes colonization of the host by the symbiotic
30 dinoflagellate *Symbiodinium minutum*. Blocking TSR domains led to decreased colonization
31 success, while adding exogenous TSRs resulted in a ‘super colonization’. Furthermore, gene
32 expression of TSR proteins was highest at early time-points during symbiosis establishment. Our
33 work characterizes the diversity of cnidarian TSR proteins and provides evidence that these
34 proteins play an important role in the establishment of cnidarian-dinoflagellate symbiosis.

35

36 **Introduction**

37

38 Host-microbe interactions, both beneficial and detrimental, are ancient and ubiquitous, and are
39 mediated by a myriad of molecular and cellular signalling events between the partners. Hosts are
40 under selective pressures to develop recognition mechanisms that tolerate beneficial symbionts
41 and destroy negative invaders, while microbes evolve to successfully invade and either benefit or
42 exploit their hosts (Eberl, 2010, Bosch and McFall-Ngai, 2011). Cnidarian-dinoflagellate
43 mutualisms, such as those that form coral reefs, are one such host-microbe interaction for which
44 we are just beginning to uncover the molecular conversations between partners that result in the
45 establishment and maintenance of a healthy partnership (Davy et al., 2012). Most cnidarian-
46 dinoflagellate partnerships are established anew with each cnidarian host generation. The
47 photosynthetic dinoflagellates (*Symbiodinium* spp.) are taken from the environment into host
48 gastrodermal cells *via* phagocytosis and, instead of being digested, the symbionts persist and
49 colonize the host.

50

51 Discovery-based, high-throughput ‘omics techniques have previously been employed to uncover
52 candidate genes and pathways that could play a role in inter-partner recognition and regulation
53 processes in cnidarian-dinoflagellate symbioses (Meyer and Weis, 2012, Mohamed et al., 2016).
54 Two such transcriptomic studies comparing expression patterns of symbiotic and aposymbiotic
55 individuals of the sea anemone species *Anthopleura elegantissima* and *Aiptasia pallida*
56 (Rodriguez-Lanetty et al., 2006, Lehnert et al., 2014), started us down a path to an in-depth
57 examination of thrombospondin-type-1-repeat (TSR)-domain-containing proteins (hereafter
58 referred to as TSR proteins) in both partners of the symbiosis. Both studies found significant
59 upregulation of a homologue to a scavenger receptor type B1 (SRB1) in symbiotic anemones.
60 The structure and diversity of SRB1s have now been characterized in a variety of cnidarians,

61 including *A. elegantissima* and *A. pallida* (Neubauer et al., 2016). SRB1s function in innate
62 immunity in metazoans in a variety of ways, including, in mammals, activation of the
63 tolerogenic, immunosuppressive transforming growth factor beta (TGF β) pathway (Asch et al.,
64 1992, Masli et al., 2006, Yang et al., 2007). When the TSR domains of the extracellular matrix
65 glycoprotein thrombospondin bind to CD36, latent TGF β is converted to its active form, which
66 in turn launches tolerogenic pathways downstream. Subsequent studies in another sea anemone
67 model system, *A. pallida*, demonstrated a role for TGF β in the regulation of cnidarian-
68 dinoflagellate symbioses (Detournay et al., 2012). This warranted further examination of genes
69 related to TGF β pathway activation and turned our focus to thrombospondins.

70
71 Our initial search for thrombospondin and other TSR protein homologues revealed a rich
72 literature on thrombospondin-related anonymous proteins (TRAPs) that play important roles in
73 apicomplexan endoparasites, such as when *Plasmodium* attaches to and invades mammalian host
74 cells (Kappe et al., 1999, Vaughan et al., 2008, Morahan et al., 2009). Specifically, the
75 WSPCSVTCG motif (Figure 1) within the TRAP TSR binds sulfated glycoconjugates on host
76 cells (Morahan et al., 2009). This piqued our interest in TSRs even more, because apicomplexans
77 and dinoflagellates are sister taxa within the alveolates (Burki et al., 2008, Adl et al., 2012).
78 There is therefore the potential for homologous strategies of symbiont invasion and persistence
79 in hosts that spurred our interest in a deeper investigation of TSR homologues within
80 *Symbiodinium*, as well as within host cnidarians.

81
82 The large TSR protein superfamily includes mammalian thrombospondins (depicted in Figure 1),
83 and many proteins in metazoans and other eukaryotes (Adams and Tucker, 2000, Tucker, 2004).
84 The superfamily is composed of secreted and transmembrane proteins with a large array of
85 functions involving protein-protein and other steric interactions. TSR superfamily members are
86 diverse, suggesting that the highly-conserved TSR domain has been duplicated and shuffled
87 numerous times among superfamily members. For example, 41 human genes contain one or
88 more TSR domain copies (Silverstein, 2002), while there are 27 and 14 TSR superfamily
89 members in *C. elegans* and *Drosophila*, respectively (Tan et al., 2002). The TSR domain consists
90 of approximately 60 amino acids (Figure 1), with several highly conserved motifs and five or six
91 conserved cysteine residues that participate in disulfide bridge formation and domain folding
92 (Adams and Lawler, 2011).

93
94 Thrombospondins were originally characterized in mammals. They are extracellular, multi-
95 domain, calcium-binding glycoproteins that play pleiotropic tissue-specific roles involving
96 interactions with cell surfaces, cytokines and the extracellular matrix (Adams and Lawler, 2004).
97 Protein-protein interactions involving the TSR domain, including binding to SRB1/CD 36 (see
98 Figure 1), are central to thrombospondin protein function. A systematic search for TSR proteins
99 across the Cnidaria has not been conducted to date. However, a study of vertebrate
100 thrombospondin protein homologues in *Nematostella vectensis* found that, although most of the

101 multi-domain architecture is present, crucially, the three TSR domains are missing (thus adding a
102 confusing naming problem to the categorization of these genes) (Bentley and Adams, 2010,
103 Tucker et al., 2012).

104

105 There is, however, growing evidence that cnidarians possess numerous genes that contain TSR
106 domains. Two rhamnospondin genes with eight TSR domains were identified in the colonial
107 hydroid *Hydractinia symbiolongicarpus* that are expressed in the hypostome of feeding polyps
108 and were proposed to function in microbe binding (Schwarz et al., 2007). A study in *Hydra*
109 *oligactis* also demonstrated high expression of several genes for TSR proteins in the hypostome
110 and proposed potential functions in nerve net development or defense (Hamaguchi-Hamada et
111 al., 2016). Within anthozoans, several TSR proteins were identified in two species of corals,
112 *Acropora palmata* and *Montastraea faveolata* (Schwarz et al., 2008), and in a study identifying
113 candidate symbiosis genes across ten cnidarian species (Meyer and Weis, 2012). Therefore,
114 while a number of studies have focused on characterization and localization of cnidarian TSR
115 proteins, their proposed functions have not yet been investigated.

116

117 The aim of this study was to characterize and compare the TSR protein repertoire of seven
118 cnidarian species (six symbiotic, one non-symbiotic) and two symbiotic dinoflagellate species, to
119 identify putative ligands for SRB1/CD36 in host sequence resources and TRAP-like proteins in
120 the *Symbiodinium* genome. Using six anthozoan genomic and transcriptomic resources, we
121 compared vertebrate TSR proteins of known function with the cnidarian TSR repertoire. We
122 investigated the presence of known binding motifs and their conservation within the cnidarian
123 TSR domains. In addition, we explored the function of TSR proteins in cnidarian-dinoflagellate
124 symbiosis, using the sea anemone *A. pallida*, a globally-adopted model system for the study of
125 this symbiosis (Weis et al., 2008, Goldstein and King, 2016). We tested the hypothesis that TSR
126 proteins are involved in symbiont colonization of the host during onset of symbiosis, and
127 whether the proteins of interest are of host or symbiont origin. Functional studies were
128 performed in which TSR-domain function was blocked, or exogenous TSRs were added to
129 determine the effect on colonization levels at the onset of symbiosis. Overall, we describe a
130 diverse TSR protein repertoire in anthozoans that contains homologues to known vertebrate
131 proteins in addition to novel domain combinations. In addition, we provide functional evidence
132 for the importance of host-derived TSR proteins in the establishment of the cnidarian-
133 dinoflagellate symbiosis.

134

135 **Results**

136

137 *Cnidarian TSR proteins*

138 The overall numbers of TSR proteins identified from the four genomes, *N. vectensis*, *A. pallida*
139 *A. digitifera*, and *S. pistillata* were much higher than those identified from transcriptomes.
140 Searches revealed a rich and diverse repertoire of TSR proteins within the seven anthozoan

141 species, when compared to mammalian TSR superfamily members of known function; the
142 largest groups identified were the ADAMTS metalloproteases and the properdin-like TSR-only
143 proteins (Figure 2). Putative thrombospondins with similar domain structure to human
144 thrombospondins 3, 4 and 5 were identified in all species. None of the cnidarian resources
145 searched contained a thrombospondin-like protein with TSR domains. Large numbers of TSR-
146 only proteins were identified in comparison to those known in mammals, where complement
147 factor properdin is the only example of a protein containing only TSR repeats aside from a signal
148 sequence. TSR protein sequences containing novel protein domain architecture were also
149 identified, including those with astacin metalloproteases, von Willebrand factors (VWAs),
150 trypsin, *Stichodactyla helianthus* K⁺ channel toxin (ShK) domains and immunoglobulin domains
151 (Figure 2).

152

153 *Analysis of potential binding sites and conserved motifs in cnidarian TSR domains*

154 TSR domains taken from a selection of identified cnidarian TSR proteins, show very strong
155 amino acid sequence homology to the second TSR repeat in the human thrombospondin 1
156 protein (Fig 2-S1). Features contributing to the three-dimensional folded protein described from
157 the crystal structure of the TSR repeat of human thrombospondin 1 (Tan et al., 2002) are present
158 in the cnidarian TSRs, including: (1) six cysteine residues, shown to form disulfide bridges; (2)
159 three tryptophan residues forming the WXXWXXW motif which participates in protein and
160 glycosaminoglycan binding sites (GAG binding); and (3) polar residues (such as arginine, lysine
161 and glutamine) present in the RXRXR motif, forming salt bridges with other polar residues that
162 aid in folding. In addition, all sequences contain the CSVTG and GVQTRXR motifs, which
163 bind SRB1/CD36 (Zhang and Lawler, 2007).

164

165 *TSR proteins in Symbiodinium minutum and S. microadriaticum*

166 Searches of the *S. minutum* genome identified 175 contigs containing TSR domains, however
167 none of the predicted proteins contained VWA domains (Figure 3). TSRs were alone or in
168 repeats of up to 16. In contrast, most apicomplexan TSR protein sequences possess one or more
169 VWA domains and all have a C-terminal transmembrane domain. Searches of the *S.*
170 *microadriaticum* genome revealed similar results and included proteins containing only the TSR
171 domains in repeats up to 20. An alignment of TSR domains, including those from apicomplexan
172 TRAP proteins, human thrombospondins 1 and 2, *S. minutum*, *S. microadriaticum* and two
173 cnidarian TSR proteins is shown in Figure 3-S1. *S. minutum* TSRs have five or six cysteines, a
174 variation that is consistent with apicomplexan TRAP proteins (Morahan et al., 2009). The
175 CD36/SRB1 but not the GAG-binding sites are well conserved in *S. minutum* sequences. In
176 contrast, *S. microadriaticum* TSR domains contain 6 cysteines and are more similar to human
177 and cnidarian TSRs than apicomplexan TSR domains.

178

179 *Evidence of TSR domain proteins in host but not symbiont*

180 Anti-human TSR labelled two bands of 40 and 47 kDa in immunoblot analysis of homogenates
181 from symbiotic *A. pallida* protein and a single band at 40 kDa in aposymbiotic *A. pallida* (Figure
182 4A, 4-S1). Immunofluorescence of *S. minutum* using anti-human TSR showed label on freshly
183 isolated but not cultured cells. Dil lithophytic membrane stain labelled freshly isolated but not
184 cultured *S. minutum* cells (Figure 4, 4-S2). Likewise, anti-TSR signal was absent from cultured
185 *S. minutum* cells (Figure 4B) but appeared around the outside of freshly-isolated *S. minutum* cells
186 (Figure 4C), suggesting that it labels the host symbiosome membrane complex and/or host
187 material associated with the freshly isolated cells. Immunofluorescent labelling of symbiotic
188 anemone tentacle cryosections showed antibody label in host gastrodermal tissue when in close
189 association with resident symbionts (Figure 4D, E). Secondary antibody-only and IgG controls
190 showed no labeling (Figure 4F).

191
192

193 *Blocking TSR domains inhibits symbiont uptake by host anemones*

194 Incubation of aposymbiotic anemones with anti-human TSR prior to and during symbiont
195 inoculation resulted in strong and statistically significant (mixed effects ANOVA F(2, 24) =
196 16.55, p < 0.0001) inhibition of host colonization by *S. minutum* (Figure 5A). Levels of
197 colonization stayed very low throughout the treatment period, rising to only 1.26 ± 0.86%. In
198 contrast, anemones incubated in both the FSW and IgG antibody controls showed moderate rates
199 of colonization for the first 72 h, but a dramatic increase thereafter to 18.1 ± 2.65% and 17.8 ±
200 2.56 %, respectively, by 120 h post-inoculation.

201

202 *Addition of exogenous human thrombospondin-1 results in ‘super colonization’ of hosts by
203 symbionts*

204 Addition of exogenous human thrombospondin-1 protein increased the rate of host colonization
205 by symbionts. Anemones pre-treated with thrombospondin-1 showed markedly increased (mixed
206 effects ANOVA F(1, 16) = 59.36, p < 0.0001) colonization success compared to FSW controls
207 (Figure 5B). Colonization success after 48 h was 8.05 ± 0.98% in the thrombospondin-1
208 treatment compared to 1.18 ± 0.28% in the FSW treatment. By 96 h post-inoculation,
209 colonization success had risen to 25.1 ± 2.6% in the thrombospondin-1 treatment compared to just
210 9.87% ± 2.4% in the FSW control. By the end of the experiment, at 120 h post-inoculation,
211 colonization levels in control animals had almost caught up to those in treatment ones,
212 suggesting that the stimulatory impact of thrombospondin-1 was most pronounced during the
213 first 96 h of symbiosis establishment.

214

215 *Addition of exogenous *A. pallida* TSR peptide fragments during inoculation increases
216 colonization success*

217 As with human thrombospondin-1, pre-treating anemones with short synthetic *A. pallida* TSR
218 peptides resulted in increased colonization success (mixed effects ANOVA F(2, 24) = 69.46, p <
219 0.0001; Figure 5C). At 48 h post-inoculation, symbiont levels were higher in anemones pre-

treated with either peptide (Peptide 1: $11.14 \pm 1.1\%$; Peptide 2: $11.78 \pm 0.9\%$) compared to the FSW-only controls ($2.08 \pm 0.29\%$). After 48 h, colonization levels in the Peptide 2 treatment were consistently higher than in the Peptide 1 treatment. This difference was particularly apparent at 72 h, where colonization levels in anemones in the Peptide 2 treatment were 5% higher than in Peptide 1 ($20.2 \pm 1.4\%$ and $15.11 \pm 1.98\%$, respectively). The peptide treatments showed the largest increase relative to the FSW control at 96 h, with $18.8 \pm 1.3\%$ and $20.9 \pm 1.68\%$ colonization for Peptides 1 and 2, respectively, compared to only $6.15 \pm 0.75\%$ for the FSW control. However, as in the thrombospondin-1 treatment, by the end of the experiment at 120 h, colonization in the control animals had reached levels similar to those in the peptide-treated anemones, suggesting once again that the impact of TSR peptides was most pronounced early in the colonization process.

231

232 *Ap_Sema-5 expression increases at early time-points during the onset of symbiosis*

To investigate the specific TSR proteins involved in the onset of symbiosis, gene expression of two sequences obtained from the bioinformatics searches of the *A. pallida* genome was measured using quantitative PCR (qPCR). The first sequence, *Ap_Sema5* (AIPGENE5874) has a domain structure similar to the vertebrate semaphorin-5 sequence with an N-terminal Sema domain and C-terminal TSR. This sequence was selected for further investigation due to its role in tumor cell motility and invasion through modifications to the actin cytoskeleton (Li and Lee, 2010), which suggests it could play a role in cytoskeletal rearrangements during symbiont uptake. The second sequence, *Ap_Trypsin-like* (similar to AIPGENE 1852), represents a novel domain combination as it possesses two N-terminal ShK domains, four TSR domains, and a C-terminal trypsin domain. The peptide used in the functional experiments described above was designed specifically to this sequence, therefore making it an interesting target for further investigation. Furthermore, in the genome searches, a similar sequence was found in symbiotic species, but not the non-symbiotic *Nematostella vectensis*, suggesting this protein may play a role in symbiosis. Quantitative PCR results revealed similar expression trends for both *Ap_Sema5* and *Ap_Trypsin* during the onset of symbiosis (Figure 6). *Ap_Sema5* showed a significant upregulation at 12 h post-inoculation (estimate: -2.26, 95% c.i.: [-3.52; -1.01], $p = 0.0072$) in the inoculated compared to aposymbiotic treatment, but by 72 h post-inoculation it was significantly downregulated (estimate: 1.98, 95% c.i.: [0.73; 3.23], $p = 0.015$). *Ap_Trypsin-like* displayed a downward trend in expression during the establishment of symbiosis (ANOVA, $F(1, 10) = 5.90$, $p = 0.036$), however individual pairwise comparisons were not significantly different (see Supplementary Source Code File 1 for detailed outputs of individual estimates and test statistics, including all pairwise comparisons at individual time-points).

255 **Discussion**

256

257 *Bioinformatic searches reveal a diversity of anthozoan TSR proteins*

258 Bioinformatic searches revealed a notable diversification of TSR-only proteins. This suggests
259 that TSR proteins can be added to the growing list of immunity genes in cnidarians that are
260 greatly diversified compared to their counterparts in vertebrate genomes. These include
261 expansions of toll-like receptors in *A. digitifera*, ficolin-like proteins in *A. pallida*, NOD-like
262 receptors in *Hydra magnipapillata* and *A. digitifera*, and scavenger receptors in a variety of
263 cnidarians (Lange et al., 2011, Shinzato et al., 2011, Hamada et al., 2013, Baumgarten et al.,
264 2015, Neubauer et al., 2016). It has been hypothesized that such an expanded repertoire in basal
265 metazoans is an alternate evolutionary strategy to vertebrate adaptive immunity that would
266 enable complex reactions to, and management of, their microbiomes (Hamada et al., 2013).

267
268 The TSR-only repertoire expansion is of particular interest because these sequences are similar
269 to the vertebrate complement protein properdin. This protein is known to have two interrelated
270 functions that may be of particular relevance to the establishment of the cnidarian-dinoflagellate
271 symbiosis. First, properdin can act as a pattern recognition receptor (PRR), detecting microbe-
272 associated molecular patterns (MAMPs) on invading microbes and triggering phagocytosis of
273 microbes directly. Secondly, it can participate in the complement system alternative pathway,
274 where it activates and stabilizes the proteolytic C3 convertase complex, which attaches to the
275 surface of invading microbes and hence marks them for phagocytosis and/or lysis (Hourcade,
276 2006, Spitzer et al., 2007). There is growing functional evidence that the complement system,
277 which is classically thought to function in defense against pathogens, also plays a role in the
278 onset and regulation of cnidarian-dinoflagellate symbiosis (Kvennefors et al., 2008, Kvennefors
279 et al., 2010, Baumgarten et al., 2015, Poole et al., 2016). Therefore, a testable hypothesis is that
280 cnidarian TSR-only proteins function in a similar manner to vertebrate properdin, as either a
281 PRR to recognize *Symbiodinium* or to interact with complement proteins to promote
282 phagocytosis of symbionts. A recent transcriptomic study indicated that there was decreased
283 expression of a transmembrane domain-containing-TSR-only protein in *A. pallida* larvae during
284 the later stages of symbiosis establishment when compared to aposymbiotic larvae (Wolfowicz et
285 al., 2016). Therefore, it is possible that this protein may serve as a PRR, with a high level of
286 expression in aposymbiotic larvae and during inter-partner surface recognition, but decreased
287 expression after phagocytosis.

288
289 We characterized a large repertoire of cnidarian ADAMTS metalloprotease-like proteins. The
290 TSR domains within these cnidarian proteins are highly conserved and functional motifs are
291 intact, including the tryptophan glycosaminoglycan-binding (GAG) motif ‘WXXW’, and
292 scavenger receptor binding motifs ‘CSVTCG’ and ‘GVITRIR’ (Adams and Tucker, 2000,
293 Silverstein, 2002). In humans, the metalloprotease ADAMTS 13 binds to SRB1 (Davis et al.,
294 2009), and in *C. elegans* an ADAMTS protein (AD-2) is responsible for initiating the TGF β
295 pathway, regulating body growth and maintaining cuticle formation (Fernando et al., 2011). It is
296 therefore conceivable that an ADAMTS-like TSR protein is involved in promoting tolerance in
297 the cnidarian-dinoflagellate symbiosis.

298

299 TSR proteins containing the trypsin domain, ShK domain and the VWA domain, were present in
300 five of the six symbiotic cnidarians, the trypsin containing TSRs identified in *A. digitifera* lack
301 the ShK domain (Figure 2). The ShK domain is found in peptides that function as potassium
302 channel inhibitors and it has been proposed that proteins that include ShK in combination with
303 other domains, such as trypsin, may also modulate channel activity (Rangaraju et al., 2010).
304 Additionally, proteins with ShK or TSR domains have previously been found in nematocysts
305 (Balasubramanian et al., 2012, Rachamim et al., 2014). Therefore, ShK plus trypsin proteins are
306 likely toxin proteins that function in nematocysts and food acquisition. Interestingly, qPCR
307 results indicated that Ap_Trypsin-like has a trend of decreased expression during the
308 establishment of the symbiosis (Figure 6). Therefore, it is still unclear what role this protein
309 plays in symbiosis. This downward trend could indicate a de-emphasis by the host on food
310 capture, as it transitions to gaining nutritional support from its symbionts. A more detailed
311 comparative study would need to be performed to determine whether these sequences are truly
312 differentially distributed as a function of symbiosis.

313

314 The comprehensive search for TSR-containing thrombospondin homologues found no sequences
315 in any of the anthozoan resources examined (Figure 2). This strongly suggests that TSR-
316 containing thrombospondins are not present in cnidarians. However, searches for TSR proteins
317 within anthozoans revealed a rich diversity of TSR superfamily members, including some whose
318 domain architectures bear a strong resemblance to members in other animals and others with
319 novel domain architectures. Domain abundance and architecture show no clear pattern based on
320 symbiotic state or anthozoan phylogeny, but instead correlate to type of resource searched:
321 genomes provide better representation of TSR abundance than transcriptomes. It is likely that a
322 more accurate picture of TSR protein diversity will emerge over time as more genomes become
323 available and annotations improve.

324

325 *Symbiodinium* *TSR proteins show limited similarities to apicomplexan TRAPs*

326 Searches of both *S. minutum* and *S. microadriaticum* genomes revealed evidence of TSR
327 proteins, but none that had all of the hallmarks of the TRAP proteins in apicomplexans.
328 *Symbiodinium* TSR sequences contain a signal peptide and multiple TSR repeats, but not the
329 VWA or transmembrane domains found in most apicomplexan TRAPs (Figure 3). It is therefore
330 unlikely that *Symbiodinium* is using TSR proteins to attach to hosts via mechanisms homologous
331 to those used by apicomplexans. Expression profiles and localization studies of symbiont TSR
332 proteins in culture vs. *in hospite* could provide insight into whether these proteins are playing a
333 role in the symbiosis. Interestingly, the number of cysteines contained in the TSR domains
334 differed between the two species. *S. minutum* TSR domains contained five cysteines, similar to
335 apicomplexan TSRs. In contrast, *S. microadriaticum* TSRs contained six, similar to metazoan
336 TSRs.

337

338 *Colonization experiments implicate the TSR domain in symbiosis establishment*

339 We introduced dinoflagellates to aposymbiotic anemones that had been pre-treated to either
340 block or mimic TSR proteins. Blocking TSR domain function resulted in colonization levels
341 reduced to 1% infection and below, providing strong evidence for the involvement of TSR
342 proteins in the establishment of the symbiosis. The anti-human TSR epitope corresponds to three
343 TSR repeats and is therefore indiscriminate in its blocking effect of TSR proteins. Results
344 indicate a role for host, rather than symbiont TSR proteins in symbiosis establishment, given the
345 localization of anti-thrombospondin to host tissues, including those of aposymbiotic anemones,
346 and not the outer surface of cultured *Symbiodinium* cells (Figure 4).

347

348 Treatment of *A. pallida* with exogenous TSR domains provided further evidence for the role of
349 host TSR proteins in the early onset of the symbiosis. Due to high levels of TSR domain
350 conservation across taxa, synthetic peptides designed from TSR domains have been employed by
351 a number of studies, including determining which motifs bind to CD36 (Li et al., 1993) and
352 which *Plasmodium* TSR peptides bind to red blood cells (Calderón et al., 2008). The synthetic
353 peptide used in this study contained both the tryptophan GAG-binding motif ‘WXXW’, and
354 scavenger receptor binding motifs ‘CSVTCG’ and ‘GVXTRXR’. This result suggests that one or
355 multiples of these binding motifs are involved in successful entry to host cells by the
356 dinoflagellates.

357

358 Treatment of *A. pallida* with human thrombospondin and synthetic *A. pallida* TSR peptides
359 resulted in ‘super colonization’ by the symbionts (Figure 5B, C). These results provide evidence
360 against the hypothesis of membrane-linked host TSRs serving as PRRs to promote inter-partner
361 recognition. We suggest that exogenous TSRs would compete with membrane bound host TSR
362 PRRs for *Symbiodinium* MAMPs, and result in decreased colonization success. Instead, our
363 results support a hypothesis of TSRs enhancing symbiont colonization through steric interactions
364 with a secondary molecule(s), be it C3 convertase complex, SRB1, or some other protein that
365 promotes phagocytosis. In this case, addition of exogenous TSRs would result in binding of
366 additional secondary proteins that would in turn promote phagocytosis and result in the ‘super
367 colonization’ observed. This hypothesis is further supported by sequence data which indicate that
368 the majority of cnidarian TSR proteins lack transmembrane domains (see Supplementary File 1).

369

370 Our initial interest in the TSR domain was prompted by the search for a binding target for the
371 host cell scavenger receptor SRB1, which is upregulated in the symbiotic state of *A. pallida* and
372 another sea anemone, *A. elegantissima* (Rodriguez-Lanetty et al., 2006, Lehnert et al., 2014). In
373 other systems, SRB1-TSR interactions are implicated in promoting phagocytosis and initiating
374 the tolerance promoting TGF β pathway by activating latent TGF β protein (Khalil, 1999,
375 Murphy-Ullrich and Poczatek, 2000, Koli et al., 2001). The addition of TSR protein may have
376 dual functions, firstly to enhance phagocytosis of microbes and secondly to promote tolerance.

377 Many intracellular parasites manipulate host innate immune defence mechanisms to their own
378 advantage (Medzhitov et al., 2002).
379
380 Gene expression results also provide evidence of a role for TSR proteins at the onset of
381 symbiosis (Figure 6). Ap_Sema5 showed increased expression at early time points during onset
382 of symbiosis, but decreased expression at later time points, indicating that it may play a role in
383 initial recognition and uptake of symbionts, but not subsequent proliferation. Future experiments
384 that target earlier time points during the onset of symbiosis could provide evidence to support
385 this hypothesis. Interestingly, the decreased trend in expression at 72 h post-inoculation is similar
386 to the downregulation observed for several TSR protein genes and a non-TSR semaphorin
387 (Semaphorin-3E) in symbiotic *A. pallida* larvae five to six days post-inoculation (Wolfowicz et
388 al., 2016). Due to the pleiotropic nature of semaphorins, further investigation of the precise role
389 of Ap_Sema5 is needed. Intriguingly, however, vertebrate semaphorin-5a has been shown to
390 play a role in modifications to the actin cytoskeleton, and it therefore could function in the
391 phagocytosis of symbionts (Li and Lee, 2010). Moreover, semaphorin-5a has been shown to
392 promote cell proliferation and to inhibit apoptosis in several cancers (Sugimoto et al., 2006, Pan
393 et al., 2010, Sadanandam et al., 2010), raising the possibility that it could promote
394 immunotolerance of foreign *Symbiodinium* cells. Lastly, Ap_Sema5 could function as a PRR. In
395 vertebrates, Semaphorin-7a has previously been shown to serve as an erythrocyte receptor for a
396 *Plasmodium* TRAP protein (Bartholdson et al., 2012), where the sema domain of semaphorin-7a
397 interacts with a TSR domain in the TRAP protein, to promote invasion of host red blood cells by
398 the parasite. Overall, there are a variety of roles that Ap_Sema5 may play to promote the onset of
399 symbiosis, and future functional experiments can be used to test these.

400
401 *Concluding remarks*
402
403 Characterization of TSR proteins in cnidarians in this study has revealed a diverse repertoire of
404 genes whose functions remain to be fully described. Functional work provides another piece in
405 the complex web of inter-partner signaling that supports symbiont acquisition and presents the
406 TSR as a protein domain potentially involved in nurturing positive microbial-host interactions in
407 the cnidarian-dinoflagellate symbiosis. Studies using antibodies, proteins, peptides and qPCR to
408 explore TSR protein function in symbiosis suggest that one or more host-derived TSR proteins is
409 participating in host-symbiont communication.

410
411 Taken together, these studies point to these proteins, potentially working in concert with other
412 secondary proteins, promoting phagocytosis of symbionts and enhancing colonization success.
413 Figure 7 presents a model summarizing the evidence emerging from the immunolocalization and
414 functional experiments. Future studies should target specific TSR homologues for further
415 investigation using antibodies made against specific proteins and ideally using knockdown or
416 gene-editing technologies that would empirically test the impact of these genes on host-symbiont

417 recognition. Overall, there is mounting evidence that *Symbiodinium* cells can manipulate the
418 host's immune defenses to gain entry to, and proliferate in cnidarian cells, as occurs in parasitic
419 infections, but how these various strands of evidence ultimately tie together is still unclear and
420 requires further investigation.

421

422 Materials and Methods

423

424 Genomic and transcriptomic resources

425 To characterize the TSR protein repertoire in cnidarians, seven species with publically available
426 resources were searched. These resources were selected to capture a diversity of anthozoans,
427 with representatives from Actinaria, and the complex and robust clades of the scleractinians.
428 Additionally, species were chosen to represent a variety of symbiotic states and symbiont
429 transmission mechanisms. These included three anemone species: *A. elegantissima* (Kitchen et
430 al., 2015), *A. pallida* (Lehnert et al., 2012, Baumgarten et al., 2015) and *Nematostella vectensis*
431 (Putnam et al., 2007), and four coral species: *Acropora digitifera* (Shinzato et al., 2011),
432 *Acropora millepora* (Moya et al., 2012), *Fungia scutaria* (Kitchen et al., 2015) and *Stylophora*
433 *pistillata* (Voolstra et al., In Review). These resources were derived from various developmental
434 stages and symbiotic states (Table 1). All resources were used without manipulation, with the
435 exception of the *A. pallida* transcriptome, for which raw Illumina sequence reads for accession
436 SRR696721 were downloaded from the sequence read archive (RRID:SCR_004891) entry
437 (<http://www.ncbi.nlm.nih.gov/sra/SRX231866>) and reassembled using Trinity
438 (RRID:SCR_013048, Grabherr et al., 2011). In addition, the genomes of the symbiotic
439 dinoflagellates *Symbiodinium minutum* (ITS2 type B1) (Shoguchi et al., 2013) and *S.*
440 *microadriaticum* (Aranda et al., 2016) were searched for TSR proteins, to investigate the
441 presence of a potential TRAP-like protein.

442

443 TSR sequence searching

444 To search for cnidarian TSR proteins, databases were queried using several search strategies to
445 ensure that all sequences were recovered. BLASTp or tBLASTn searches with the second TSR
446 domain from mouse and human thrombospondin-1 protein sequences, and the consensus
447 sequence (smart00209: TSP1) from the conserved domain database (RRID:SCR_002077,
448 <http://www.ncbi.nlm.nih.gov/cdd>) as queries were performed for each resource. Keyword
449 searches using the terms TSP1, thrombospondin, ADAMTS, ADAM and SEMA were also
450 performed where genome browsers allowed keyword searches of GO, KEGG and PFAM
451 annotations. Lastly, representative *N. vectensis* sequences of each protein type (ADAMTS-like,
452 SEMA, TRYPSIN and TSR-only) were also used as queries for tBLASTn searches of the other
453 six cnidarian resources. A high e-value cutoff (1×10^{-1}) was used in the BLAST searches to
454 recover divergent sequences. All BLAST searches were performed using Geneious pro version
455 7.1.8 (RRID:SCR_010519, Kearse et al., 2012) with the exception of the *N. vectensis*, *A. pallida*
456 and *S. pistillata* genomes, for which searches were performed through the Joint Genome Institute

457 online portal (RRID:SCR_002383), NCBI (RRID:SCR_004870) and the Reefgenomics online
458 repository (RRID: SCR_015009, <http://reefgenomics.org>)(Liew et al., 2016), respectively. A list
459 of metazoan resources searched is provided in Table 1. Sequences identified are tabulated in
460 Supplementary File 1.

461

462 To confirm that the sequences obtained contained TSR domains, nucleotide sequences were
463 translated using Geneious or ExPASy translate tool (RRID:SCR_012880,
464 <http://web.expasy.org/translate/>) and then annotated using the Geneious InterProScan plugin
465 (RRID:SCR_010519, Kearse et al., 2012). All annotations were double checked using the online
466 protein domain database PfamA (RRID:SCR_004726, <http://pfam.sanger.ac.uk>), and only
467 sequences that showed significant PfamA matches to a TSR domain with an e-value of $<1\times10^{-4}$
468 were used. Sequences for each species were aligned and those that were identical or almost
469 identical (<5 aa difference in the conserved domains) were omitted from the analysis, as they
470 likely represented artefacts of assembly or different isoforms of the same protein. Sequences
471 missing a start or stop codon were removed from the analysis. Diagrammatic representations of
472 the protein domain configurations were produced using this information. Protein domain
473 architectures were grouped together according to common domains and compared to known
474 human TSR proteins (Figure 3).

475

476 *Maintenance and preparation of anemone and dinoflagellate cultures*

477 A population (not necessarily clonal) of *Symbiodinium minutum* (clade B1)-containing *A.*
478 *pallida*, originating from a local pet store, was maintained in saltwater aquaria at 26 °C at a light
479 intensity of approximately 40 $\mu\text{mol quanta m}^{-2} \text{s}^{-1}$ with a 12/12 h light/dark photoperiod, and fed
480 twice weekly with live brine shrimp nauplii. Animals were rendered aposymbiotic by incubation
481 for 8 h at 4 °C twice weekly for six weeks, followed by maintenance in the dark for
482 approximately one month. Anemones were fed twice weekly with brine shrimp, and cleaned of
483 expelled symbionts and food debris regularly.

484

485 Cultured dinoflagellates - *Symbiodinium minutum* (sub-clade B1; culture ID CCMP830 from
486 Bigelow National Center for Marine Algae and Microbiota) - were maintained in 50 ml flasks in
487 sterile Guillard's f/2 enriched seawater culture medium (Sigma, St. Louis, MO, USA).
488 Dinoflagellate cultures were maintained at 26 °C and 70 $\mu\text{mol quanta m}^{-2} \text{s}^{-1}$ with a 12/12 h
489 light/dark photoperiod. CCMP830 cultures were typed using Internal transcribed spacer 2
490 (ITS2) sequencing in 2009 and 2016 to authenticate the identity of the culture. The CCMP830
491 cultures were not axenic and therefore *Mycoplasma* contamination testing was not performed.

492

493 In preparation for experimental manipulation, individual anemones were placed in 24-well plates
494 in 2.5 ml of 1 μm -filtered seawater (FSW) and acclimated for 3-4 days, with the FSW replaced
495 daily. Well-plates containing aposymbiotic anemones were kept at 26 °C in the dark, while those
496 containing symbiotic anemones were maintained in an incubator at a light intensity of

497 approximately 40 μmol quanta $\text{m}^{-2} \text{s}^{-1}$ with a 12/12 h light/dark photoperiod. Animals were not
498 fed during the acclimation or experimental periods.

499

500

501 *Immunoblot analysis of anti-thrombospondin protein targets*

502

503 Immunoblots were performed on *A. pallida* proteins using an anti-human thrombospondin rabbit
504 polyclonal antibody. The thrombospondin antibody was made against an epitope corresponding
505 to the three TSR domains of human thrombospondin proteins 1 and 2 (Santa Cruz Biotechnology
506 Cat# sc-14013 RRID:AB_2201952). The epitope showed sequence similarity to a TSR protein
507 identified in *A. pallida* (Figure 8A). Groups of eight aposymbiotic or symbiotic anemones were
508 homogenized on ice in 1 ml homogenization buffer (50 mM Tris-HCl, pH 7.4, 300 mM NaCl, 5
509 mM EDTA) with a protease inhibitor cocktail (BD Biosciences, San Jose, CA, USA).

510 Homogenates were centrifuged at 4 °C for 15 min at 14,000 x g to pellet cell debris, supernatants
511 were decanted and protein concentrations were determined using the Bradford assay. Protein was
512 adjusted or diluted in RIPA buffer to a standard concentration of 50 μg total protein *per* well and
513 boiled for 5 min in loading dye. Proteins were resolved on a 7% SDS-PAGE gel and then
514 electrophoretically transferred overnight onto nitrocellulose membrane. After blocking with 5%
515 non-fat dry milk in TBS-Tween 20 (0.1%) for 1 h at 37°C, membranes were incubated with anti-
516 thrombospondin or an IgG isotype control, both at a dilution of 1:200, for 2 h at room
517 temperature. The blots were washed three times in TBS-Tween 20 followed by incubation in a
518 HRP-conjugate goat anti-rabbit IgG Alexa Fluor 546 secondary antibody (Molecular Probes
519 Cat# A-11030 RRID:AB_144695) at a 1:5000 dilution (0.2 $\mu\text{g ml}^{-1}$; Sigma, St. Louis, MO,
520 USA) for 1 h. Bands were detected by enhanced chemiluminescence (Millipore, Temecula, CA,
521 USA). Blots were stripped and re-probed with an actin loading control (Santa Cruz
522 Biotechnology Cat# Sc-1616 RRID:AB_630836), see Figure 4-S1 for actin control.

523

524 *Cryosectioning and immunofluorescence microscopy to localize TSR proteins*

525 Immunofluorescence was used to investigate the presence of TSR proteins on the surface of
526 dinoflagellate cells. We compared anti-human TSR binding in cultured *S. minutum* strain
527 CCMP830 to *S. minutum* cells freshly isolated from *A. pallida*. To obtain freshly-isolated
528 symbiont cells with intact symbiosome membranes, anemones were homogenized in a microfuge
529 tube with a micro-pestle and the resulting homogenate was centrifuged at a low speed (<1000
530 rpm) for 5 min to produce an algal pellet. The pellet was washed several times in FSW and re-
531 pelleted. Algal cells were re-suspended to a final concentration of 2.5×10^4 cells *per* ml. The
532 lipophilic membrane stain, Dil (1,1'-dioctadecyl-3,3,3',3'-tetramethylindocarbocyanine
533 perchlorate, DilC18(3); Molecular Probes), was used to test for the presence of putative
534 symbiosome membrane surrounding freshly isolated symbiont cells and cells taken from culture.
535 Dil was added to cells in 500 μl of FSW in a microfuge tube and gently mixed shortly before
536 small amounts of suspended cells were placed on a well slide and imaged. Both cultured and

537 freshly isolated *S. minutum* cells were incubated in the anti-human TSR conjugated to the
538 secondary antibody Alexa Fluor 546 goat anti rabbit IgG fluorescent probe (Molecular Probes
539 Cat# A-11030 RRID:AB_144695) at a 1:1000 dilution. Anti-thrombospondin and Dil labeling in
540 cells was imaged using a Zeiss LSM 510 Meta microscope through a Plan- APOCHROMAT
541 63x/1.4 Oil DIC objective lens. See Supplementary File 2 for a description of fluorescent dyes
542 and the specific excitation and emission wavelengths.

543

544 To localize TSR proteins in symbiotic and aposymbiotic anemone tissues, cryosections of
545 anemone tentacles were made using methods modified from (Dunn et al., 2007). The sections
546 were washed twice in PBS and fixed with 4% PFA for 10 min, and then washed twice in PBS.
547 Sections were then permeabilized with 0.2% Triton-X-100 in PBS for 5 min and blocked in 3%
548 BSA, 0.2% Triton-X-100 in PBS for 30 min, before incubation in the anti-human TSR rabbit
549 polyclonal antibody (described above) at a 1:200 dilution (in blocking buffer) for 4 h at 4°C.
550 Slides were subsequently washed three times for 5 min each with 0.2% Triton-X-100 in PBS at
551 rt. Alexa Fluor 546 (Molecular Probes Cat# A-11030 RRID:AB_144695) secondary antibody
552 was diluted in blocking buffer (1:150 dilution) and added to the slides for 1 h in the dark at rt.
553 Slides were washed three times in the dark for 5 min with 0.2% PBS/Triton-X-100. A drop of
554 Vectashield DAPI hard set mounting medium was then used to stain nuclei and mount cover
555 slips onto slides. Immunofluorescence was visualized using a Zeiss LSM 510 Meta microscope
556 through a Plan-APOCHROMAT 63x/1.4 Oil DIC objective lens. The fluorescence
557 excitation/emission was 556/573 nm for Alexa Fluor 546 and 543/600-700 nm for *Symbiodinium*
558 chlorophyll autofluorescence (see Supplementary File 2).

559

560 *Experimental manipulation of anemones*

561 In preparation for experimental manipulation, individual anemones were placed in 24-well plates
562 in 2.5 ml FSW and acclimated for 4 days, with FSW replaced daily. During this time,
563 aposymbiotic anemones were maintained in darkness, and symbiotic anemones were maintained
564 in an incubator at 26°C under the light regime described above. Animals were not fed during the
565 experimental period.

566

567 Aposymbiotic anemones were experimentally inoculated with *S. minutum* cells and colonization
568 success was determined by quantifying the number of symbionts present in host tissues (see
569 below). Experimental treatments were initiated 2 h prior to colonization with *S. minutum*. For
570 inoculation, cultured *S. minutum* cells were added to each well to a final concentration of 2×10^5
571 cells ml⁻¹. After incubation with dinoflagellate cells for 4 h, anemones were washed twice in
572 FSW and experimental treatments were refreshed. Well-plates were then placed back into an
573 incubator at 26°C under the light regime described above.

574

575 Addition of anti-human TSR rabbit polyclonal antibody during onset of symbiosis: To
576 investigate the effects of blocking TSR domains at the onset of symbiosis, aposymbiotic

577 anemones were incubated with the rabbit anti-human TSR polyclonal antibody as described
578 above. Anemones were incubated for 2 h prior to inoculation with *S. minutum* in anti-human
579 TSR (Santa Cruz Biotechnology Cat# sc-14013 RRID:AB_2201952), at a concentration of 0.5
580 µg antibody ml⁻¹ FSW. Control animals were given fresh FSW at the same time. For inoculation,
581 cultured *S. minutum* cells were added to each well, to a final concentration of 2 x 10⁵ cells ml⁻¹.
582 After incubation with dinoflagellate cells for 4 h, anemones were washed twice in FSW and
583 experimental treatments were refreshed. Well-plates were then placed back into an incubator at
584 26°C under the light regime described above. Anemones were sampled at 48, 72, 96 and 120 h
585 post-inoculation to measure colonization success. Colonization success was determined by
586 quantifying the number of symbionts present in host tissues (detailed below). Treatment
587 conditions of these animals were refreshed once every 24 h.

588

589 Addition of human thrombospondin-1 protein: To investigate the effect of TSR proteins on
590 dinoflagellate colonization success, soluble human thrombospondin-1 protein (thrombospondin
591 human platelet, Athens Research and Technology, #:16-20-201319) was added to aposymbiotic
592 anemones at a concentration of 25 µg ml⁻¹ FSW. All other aspects of this experiment were
593 identical to those described for the addition of anti-human TSR.

594

595 Addition of synthetic TSR peptides: To investigate whether native *A. pallida* TSR domains
596 would produce a similar effect to human thrombospondin protein, anemones were incubated in
597 synthetic TSR peptides at a concentration of 150 µg ml⁻¹ FSW. Several studies have used TSR
598 peptide fragments to investigate the binding sites of specific receptors such as SRB1 (Li et al.,
599 1993, Tolsma et al., 1993, Karagiannis and Popel, 2007, del Valle Cano et al., 2009). The
600 putative TSR domain from *A. pallida* contains multiple binding motifs - WXXWXXW,
601 CSVTCG and GVQTRLR - which are all known to bind glycosaminoglycans and class B
602 scavenger receptors in humans. Two separate peptides were designed (Figure 8B). Peptide 1 was
603 identical to TSR domain 2 from the predicted protein *A. pallida* comp25690 (taken from an *A.*
604 *pallida* transcriptome (Lehnert et al., 2012)). For Peptide 2, the cysteine residues in Peptide 1
605 were substituted with alanine residues to avoid peptide self-adhesion and hence loss of adhesion
606 to target molecules. Peptides were designed according to peptide design guidelines (at
607 www.biomatik.com version 3, RRID:SCR_008944). All other aspects of this experiment were
608 identical to those described for the addition of anti-human TSR.

609

610 *Assessing colonization success using confocal microscopy*

611 Colonization success was assessed fluorometrically with a Zeiss LSM 510 Meta confocal
612 microscope, following the methods detailed elsewhere (Detournay et al., 2012, Neubauer et al.,
613 2016). Colonization success was expressed as the percent of pixels with an autofluorescence
614 intensity above the background intensity. Each experimental treatment had a sample size of three
615 anemones *per* treatment and time-point, with percent colonization taken as a mean of three to
616 four tentacles *per* anemone. Three untreated symbiotic anemones (three to four tentacles *per*

617 anemone) were examined to determine a baseline colonization level for symbiotic anemones.
618 The sample size was limited by both the supply of anemones as well as the number of anemones
619 that could be processed for confocal microscopy at each time point.

620

621 *Statistical analysis of colonization success*

622 The statistical significance of colonization success under the treatments described above was
623 assessed using a mixed-effects analysis-of-variance model. As measures on multiple samples
624 (i.e., tentacles) *per* anemone violate independence assumptions, we treated ‘anemone’ as a
625 random effect to account for correlation among samples within anemones. Main effects included
626 time (in hours) and treatment, and their interaction was estimated to account for differences
627 between treatments at each time point. The full model can be written as:

628

$$y_{i,j} = \beta X_i + \mu_j + \epsilon_{i,j}$$

629

630 Here, $y_{i,j}$ is the logarithm of percent colonization of tentacle i within anemone j , β is a vector of
631 effects to be estimated, X is a design matrix encoding the treatment and time point, as well as
632 interaction term contrasts, μ_j is a normally distributed random effect for anemone j , and $\epsilon_{i,j}$ are
633 normally distributed residuals. Contrasts were specified between each treatment and controls at
634 each time-point to assess statistical significance of treatment effects over time, using Tukey’s
635 *post-hoc* test to account for multiple comparisons. The model was estimated using the NLME
636 package (Pinheiro et al., 2016) for the statistical computing software R (R-Core-Team, 2012)
637 (RRID:SCR_001905, www.R-project.org). All datasets and code to reproduce statistical analyses
638 and figures are given as supplementary materials (Figures 5-source data 1-6, and Supplementary
639 Source Code File 1).

640

641 *qPCR of TSR-domain-containing proteins*

642 To investigate the specific TSR proteins that are involved in the onset of symbiosis, gene
643 expression of two sequences obtained from the bioinformatics searches of the *A. pallida* genome,
644 Ap_Sema5 and Ap_Trypsin-like was measured using quantitative PCR (qPCR). First, to confirm
645 the genome assembly, primers for each sequence were designed using Primer3plus
646 (RRID:SCR_003081, <http://primer3plus.com/cgi-bin/dev/primer3plus.cgi>) to amplify
647 overlapping 700-900 bp fragments (Supplementary file 3). PCR for each primer set was
648 performed using the Go Taq Flexi kit (Promega, Madison, WI) with the following protocol:
649 94°C for 3 min, 35 cycles of 94°C for 45 s, annealing temperature for 45 s, and 72°C for 1 min,
650 followed by a final extension at 72°C for 10 min. PCR products were cleaned using the
651 QiaQuick PCR purification kit (Qiagen, Valencia CA) and sequenced on the ABI 3730 capillary
652 sequence machine in the Center for Genome Research and Biocomputing (CGRB) at Oregon

653 State University. Sequences obtained were aligned to the original genome sequence using
654 Geneious v 7.1.8 (RRID:SCR_010519, Kearse et al., 2012) to verify amplification of the correct
655 sequence and ensure that overlapping regions between fragments displayed high similarity. If a
656 region varied greatly from the genome, the region was re-sequenced for confirmation before
657 moving forward. Ap_Trypsin-like contained a region that was different than AIPGENE 1852,
658 and therefore this sequence has been submitted to GenBank (accession # KY807678). qPCR
659 primers for products between 100-200 bp with an annealing temperature of 60°C were designed
660 using Primer3 Plus (Supplementary File 4), and the products were amplified and sequenced as
661 previously described to confirm the correct amplicon. The efficiency of each primer set was
662 tested to ensure that it was at least 90%.

663
664 To investigate the expression of Ap_Sema5 and Ap_Trypsin-like at the onset of symbiosis,
665 qPCR was performed on samples from a previous experiment in which aposymbiotic specimens
666 of *A. pallida* were inoculated with *S. minutum* strain CCMP830 (Poole et al., 2016). The two
667 treatment groups used in this study were aposymbiotic animals that were inoculated with
668 symbionts ('inoc') and aposymbiotic animals that received no symbionts and remained
669 aposymbiotic for the duration of the experiment ('apo'). The animals used in this study were
670 sampled at 12, 24, and 72 h post-inoculation (n=3 for each time point and treatment
671 combination) Symbiont quantification data indicated symbionts were taken up by 24 h post-
672 inoculation and levels continued to increase between 24 and 72 hours (Poole et al., 2016). The
673 anemones were washed at 24 h and therefore the increase between 24 and 72 h can be attributed
674 to symbiont proliferation within the host. Therefore, the time points selected represent a period in
675 which symbionts were actively engaging in recognition and phagocytosis by host cells (12 and
676 24 h) and as symbionts were proliferating within the host (72 h). qPCR plates were run as
677 previously described (Poole et al., 2016) using the ABI PRISM 7500 FAST, and resulting Ct
678 values were exported from the machine. Triplicates were averaged and the expression of target
679 genes was normalized to the geometric mean of the reference genes (L10, L12, and PABP). To
680 calculate the $\Delta\Delta$ Ct, the normalized value for each sample was subtracted from the average
681 normalized value of a reference sample, the apo at each time-point. The resulting relative
682 quantities on the \log_2 scale were used for statistical analysis using R version 3.2.1
683 (RRID:SCR_001905, RCoreTeam, 2015). Identical linear models were used to test the
684 hypothesis of no significant difference in gene expression between "apo" and "inoc" anemones
685 for both genes. The model was identical to the statistical model described above, but did not
686 include a random effect. A two-way ANOVA was run to test for statistical significance of
687 treatment effects, followed by Tukey's *post hoc* test for pairwise comparisons. All datasets and
688 code to reproduce statistical analyses are given as supplementary materials (Figure 6-source data
689 1 and Supplementary Source Code File 1).

690
691
692

693 **Acknowledgements**
694 We thank Eli Meyer for the reassembly of the *A. pallida* transcriptome, Camille Paxton for
695 immunohistochemistry advice and Anne LaFlamme for providing parasitology perspectives. We
696 wish to acknowledge the Confocal Microscopy Facility at the Center for Genome Research and
697 Biocomputing at Oregon State University. This work was partially supported by a grant from the
698 National Science Foundation to VMW (IOB0919073). EFN was supported by a Commonwealth
699 Doctoral Scholarship and a Faculty of Science Strategic Research Grant from Victoria University
700 of Wellington. KT was supported on SURE Science summer fellowship from the OSU College
701 of Science.
702
703

704 **Figure Legends**

705 **Figure 1.** Schematic representation of human thrombospondin 1 protein. The three TSR
706 (Thrombospondin Structural homology Repeat) domains are depicted by three red diamonds.
707 The amino acid sequence of the second TSR sequence is shown with six conserved cysteines in
708 red. Known binding motifs and capabilities of the human thrombospondin TSR domain 2 are
709 listed and depicted in boxes. (Redrawn from (Zhang and Lawler, 2007)).

710 **Figure 2.** Domain architecture of cnidarian TSR super-family proteins compared to known
711 vertebrate TSR-domain-containing proteins.

712
713 **Figure 3.** Schematic representation of members of the thrombospondin gene family in
714 apicomplexan parasites. Apicomplexan TRAP proteins are shown in orange and TSR-domain-
715 containing proteins from the dinoflagellates *Symbiodinium minutum* and *S. microadriaticum* are
716 shown in green.

717
718 **Figure 4.** Immuno-analyses using anti-thrombospondin show evidence of TSRs in symbiotic
719 anemone host tissues. **(A)** Immunoblots of symbiotic (SYM) and aposymbiotic (APO) *A. pallida*
720 label bands at 40 and 47 kDa in symbiotic anemones and a single band at 40 kDa in
721 aposymbiotic anemones. **(B, C)** Confocal images of dinoflagellate cells taken from (B) culture or
722 (C) freshly isolated cells taken from *A. pallida* homogenates. A fluorescent probe conjugated to
723 anti-human thrombospondin does not label cells from culture (B) but strongly labels host cell
724 debris and/or membranes associated with freshly isolated cells (C). **(D, E)** Confocal images of
725 cryosections from symbiotic *A. pallida* gastrodermal tissue stained with anti-thrombospondin at
726 lower (D) and higher (E) magnification. Anti-thrombospondin labelling is evident in host tissues
727 surrounding symbionts. **(F)** Confocal image of control anemone cryosections incubated with
728 secondary antibody-only. Not anti-thrombospondin labeling is evident. Green = anti-
729 thrombospondin, Red = algal autofluorescence, blue = DAPI stain of host and symbiont nuclei.

730
731 **Figure 5.** Kinetics of recolonization after antibody and peptide treatments. **(A)** Anemones pre-
732 incubated in an anti-human thrombospondin (green) show decreased colonization success
733 compared FSW-only (light blue) and IgG (orange) controls. Inset: confocal images show
734 representative tentacle slices at 72 h post-inoculation. **(B)** The addition of exogenous human
735 thrombospondin-1 (purple) significantly increased the colonization rate during colonization,
736 compared to control anemones in FSW (blue). Inset confocal images show representative
737 tentacle slices at 96 h post-inoculation. **(C)** The effect of synthetic TSR peptides 1 (blue) and 2
738 (orange) on colonization rates compared to the control anemones in FSW. Anemones treated
739 with both peptides 1 and 2 showed increased uptake of algae during colonization. Statistical
740 significance of treatment effects was assessed using mixed effects models, with contrasts
741 calculated between individual treatments and FSW at each time-point; ***p < 0.001; *p < 0.05;
742 p < 0.1.

743 **Figure 6.** Gene expression of Ap_Sema5 and Ap_Trypsin-like at the onset of symbiosis. The
744 relative quantities from qPCR on the log₂ scale are shown for animals that were inoculated with
745 symbionts ('Inoc'; solid line) and those that remained aposymbiotic ('Apo'; dashed line). Bars
746 represent means ± SE (n = 3) and stars represent significantly different levels of expression
747 between the inoc and apo treatments at a particular time point (two-way ANOVA, Tukey's *post
748 hoc* test). * p < 0.05, ** p < 0.01

749

750 **Figure 7.** Model summarizing the evidence emerging from immunolocalization and functional
751 experiments. Gastrodermal cell A depicts an aposymbiotic host cell in the process of symbiont
752 acquisition. Results indicate that the addition of soluble TSR proteins promotes and enhances
753 symbiont colonization. We suggest that secreted host TSR proteins may interact with MAMPs
754 and/or secondary proteins to promote tolerance and initiate phagocytosis. Peptide experiments
755 provide evidence against the hypothesis that membrane-linked host TSRs are serving as PRRs to
756 promote inter-partner recognition; we hypothesize that host TSR proteins are secreted rather than
757 membrane-anchored (see discussion text for further explanation). Gastrodermal cell B depicts a
758 symbiotic host cell. Fluorescence microscopy suggests that TSR proteins are expressed within
759 the host-derived symbiosome membrane complex and are concentrated around the symbionts
760 within host gastrodermal tissue.

761

762 **Figure 8.** Sequence information for thrombospondin antibody and TSR peptide fragments used
763 in this study. **(A)** Alignment of the second TSR domains from human thrombospondin 1 and TSR
764 proteins from the anemone *Aiptasia pallida* and the dinoflagellate *Symbiodinium minutum*. In red
765 are the binding sites for glycosaminoglycans (GAGs) and CD36; greyscale indicates the %
766 identity of the three sequences. Pink annotation indicates the TSR peptide sequence covering all
767 three binding domains; inset are the synthetic peptide sequences for experimental peptides. In
768 Peptide 2, the cysteine residues were replaced with alanine residues, as shown in red. **(B)** A
769 section of the antibody-binding region of the human thrombospondin 1/2 antibody (H-300, sc-
770 14013 from Santa Cruz Biotechnology), aligned to a TSR protein fragment from *Aiptasia* sp.

771

772 **Legends for Supplementary Material**

773

774 Figure 2-figure supplement 1: The TSR domain is very well conserved from cnidarians up to
775 humans, with binding motifs for glycosaminoglycans (GAGs) and the type B scavenger
776 receptors, CD36/SRB1. All three-dimensional folding sites are present as described by Tan et al.
777 (2002) for the crystal structure of human TSP1 TSR2. Six conserved cysteine residues are
778 highlighted in yellow and form 3 disulfide bridges (C1-C5, C2-C6 and C3-C4). Three conserved
779 tryptophan residues are shown in blue boxes and mark the 'WXXW' protein-binding motif.
780 Amino acids that form the R layers are marked with purple boxes, and pairings forming 3 R
781 layers are as follows: R3-R4, R2-R5 and R1-R6. The B strands are annotated at the bottom in

782 blue strands A, B and C. Please refer to Tan et al. (2002) for a more detailed explanation of the
783 three-dimensional folding.

784

785 Figure 3-figure supplement 1: TSR domain alignment compares apicomplexan TRAP TSR
786 domains with TSR domains from the dinoflagellates *Symbiodinium minutum* and *S.*
787 *microadriaticum*, TSR 2 from human TSP1, and ADAMTS-like TSR domains from the
788 anemones *Nematostella vectensis* and *Aiptasia pallida*. Positioning and absence of specific
789 cysteine residues (colored yellow) in TRAP and *Symbiodinium* TSRs will result in different
790 patterns of disulfide bonds and three-dimensional folding. Binding sites for glycosaminoglycans
791 (GAGs) and the scavenger receptors CD36/SRB1 (annotated in red) are somewhat conserved.

792

793 Figure 4-figure supplement 1. A: Actin control for immunoblot blot in Figure 4

794

795 Figure 4-figure supplement 2. Lipophilic membrane staining of dinoflagellate cells using Dil.
796 Lipophilic membrane stain Dil was absent from (A) cultured algae but present in (B) freshly
797 isolated symbionts. This is evidence of the presence of a symbiosome membrane surrounding
798 freshly isolated symbionts.

799

800 Figure 5-source data 1. Source data used for statistical analyses described in results and depicted
801 in Figure 5A: Long-form table with experimental results described in the results section *Blocking*
802 *TSR domains inhibits symbiont uptake by host anemones* and shown in Figure 5A. Treatments
803 labels are FSW: Filtered Sea Water, anti-TSR: anti-human thrombospondin antibody, IgG: IgG
804 control.

805

806 Figure 5-source data 2. Summary statistics (mean and s.e.) displayed in Figure 5A. Summary
807 statistics for results in section *Blocking TSR domains inhibits symbiont uptake by host anemones*
808 as shown in Figure 5A.

809

810 Figure 5-source data 3. Source data used for statistical analyses described in results and depicted
811 in Figure 5B. Long-form table with experimental results described in the results section *Addition*
812 *of exogenous human thrombospondin-1 results in ‘super colonization’ of hosts by symbionts* and
813 shown in Figure 5B. Treatments labels are FSW: Filtered Sea Water, Hs-TSR: *Homo sapiens*
814 exogenous TSR protein treatment.

815

816 Figure 5-source data 4. Summary statistics (mean and s.e.) displayed in Figure 5B. Summary
817 statistics for results in section *Addition of exogenous human thrombospondin-1 results in ‘super*
818 *colonization’ of hosts by symbionts* as shown in Figure 5B.

819

820 Figure 5-source data 5. Source data used for statistical analyses described in results and depicted
821 in Figure 5C. Long-form table with experimental results described in the results section *Addition*

822 *of exogenous A. pallida TSR peptide fragments during inoculation increases colonization success*
823 and shown in Figure 5C.

824
825 Figure 5-source data 6. Summary statistics (mean and s.e.) displayed in Figure 5C. Summary
826 statistics for results in section *Addition of exogenous A. pallida TSR peptide fragments during*
827 *inoculation increases colonization success* as shown in Figure 5C.

828
829 Figure 6-source data 1. Source data used for statistical analyses described in results and depicted
830 in Figure 6. Long-form table with experimental results described in the results section *Ap_Sema-*
831 *5 expression increases at early time-points during the onset of symbiosis* and shown in Figure 6.

832
833 Supplementary File 1: Tabulated TSR sequences identified from searches of six cnidarian and
834 two dinoflagellate resources and TSR sequences from other organisms used in this study.
835 Sequences are sorted by protein type or source organism.

836
837 Supplementary File 2: Summary of fluorescent dyes and their excitation and emission
838 wavelengths used for confocal microscopy

839
840 Supplementary File 3. Primers for initial PCR of TSR sequences.

841
842 Supplementary File 4. Primers used for qPCR of Ap_Sema5 and Ap_Trypsin-like amplicons.

843
844 Supplementary Source Code File 1. R-code for statistical analyses performed for data displayed
845 in Figures 5 and 6.

849

850 **Table 1.** Anthozoan and Dinoflagellate resources

Organism	Family	Developmental stage	Symbiotic state	Data type	Publication
<i>Nematostella vectensis</i>	Edwardsiidae	Larvae	Non-symbiotic	Genome	Putnam et al. 2007
<i>Anthopleura elegantissima</i>	Actiniidae	Adult	Aposymbiotic	Transcriptome	Kitchen et al. 2015
<i>Aiptasia pallida</i>	Aiptasiidae	Adult	Aposymbiotic	Transcriptome	Lehnert et al. 2012
<i>Aiptasia pallida</i>	Aiptasiidae	Adult	Symbiotic	Genome	Baumgarten et al. 2015
<i>Acropora digitifera</i>	Acroporidae	Sperm	Symbiotic	Genome	Shinzato et al. 2011
<i>Acropora millepora</i>	Acroporidae	Adult and Larvae	Symbiotic	Transcriptome	Moya et al. 2012
<i>Fungia scutaria</i>	Fungiidae	Larvae	Aposymbiotic	Transcriptome	Kitchen et al. 2015
<i>Stylophora pistillata</i>	Pocilloporidae	Adult	Symbiotic	Genome	Voolstra et al. In review
<i>Symbiodinium minutum</i>	Symbiodiniaceae	culture ID Mf1.05b.01	Dinoflagellate culture	Genome	Shoguchi et al. 2013
<i>Symbiodinium microadriaticum</i>	Symbiodiniaceae	strain CCMP2467	Dinoflagellate culture	Genome	Aranda et al. 2016

851

852

- 853 **References**
- 854
- 855 ADAMS, J. C. & LAWLER, J. 2004. The thrombospondins. *International Journal of*
856 *Biochemistry and Cell Biology*, 36, 961-968.
- 857 ADAMS, J. C. & LAWLER, J. 2011. The Thrombospondins. *Cold Spring Harbor Perspectives*
858 *in Biology*, 3.
- 859 ADAMS, J. C. & TUCKER, R. P. 2000. The thrombospondin type 1 repeat (TSR) superfamily:
860 Diverse proteins with related roles in neuronal development. *Developmental Dynamics*,
861 218, 280-299.
- 862 ADL, S. M., SIMPSON, A. G. B., LANE, C. E., LUKES, J., BASS, D., BOWSER, S. S.,
863 BROWN, M. W., BURKI, F., DUNTHORN, M., HAMPL, V., HEISS, A.,
864 HOPPENRATH, M., LARA, E., LE GALL, L., LYNN, D. H., MCMANUS, H.,
865 MITCHELL, E. A. D., MOZLEY-STANDRIDGE, S. E., PARFREY, L. W.,
866 PAWLOWSKI, J., RUECKERT, S., SHADWICK, L., SCHOCH, C. L., SMIRNOV, A.
867 & SPIEGEL, F. W. 2012. The revised classification of Eukaryotes. *Journal of Eukaryotic*
868 *Microbiology*, 59, 429-493.
- 869 ARANDA, M., LI, Y., LIEW, Y., BAUMGARTEN, S., SIMAKOV, O., WILSON, M., PIEL, J.,
870 ASHOOR, H., BOUGOUFFA, S., BAJIC, V. B., RYU, T., RAVASI, T., BAYER, T.,
871 MICKLEM, G., KIM, H., BHAK, J., LAJEUNESSE, T. C. & VOOLSTRA, C. R. 2016.
872 Genomes of coral dinoflagellate symbionts highlight evolutionary adaptations conducive
873 to a symbiotic lifestyle. *Scientific Reports*, 6.
- 874 ASCH, A. S., SILBIGER, S., HEIMER, E. & NACHMAN, R. L. 1992. Thrombospondin
875 sequence motif (CSVTCG) is responsible for CD36 binding. *Biochemical and*
876 *Biophysical Research Communications*, 182, 1208-1217.
- 877 BALASUBRAMANIAN, P. G., BECKMANN, A., WARNKEN, U., SCHNÖLZER, M.,
878 SCHÜLER, A., BORNBERG-BAUER, E., HOLSTEIN, T. W. & ÖZBEK, S. 2012.
879 Proteome of Hydra nematocyst. *Journal of Biological Chemistry*, 287, 9672-9681.
- 880 BARTHOLDSON, S. J., BUSTAMANTE, L. Y., CROSNIER, C., JOHNSON, S., LEA, S.,
881 RAYNER, J. C. & WRIGHT, G. J. 2012. Semaphorin-7A is an erythrocyte receptor for
882 *P. falciparum* merozoite-specific TRAP homolog, MTRAP. *PLoS Pathog*, 8, e1003031.
- 883 BAUMGARTEN, S., SIMAKOV, O., ESHERICK, L. Y., LIEW, Y. J., LEHNERT, E. M.,
884 MICHELL, C. T., LI, Y., HAMBLETON, E. A., GUSE, A., OATES, M. E., GOUGH, J.,
885 WEIS, V. M., ARANDA, M., PRINGLE, J. R. & VOOLSTRA, C. R. 2015. The genome
886 of *Aiptasia*, a sea anemone model for coral symbiosis. *Proceedings of the National*
887 *Academy of Sciences*, 112, 11893-11898.
- 888 BENTLEY, A. A. & ADAMS, J. C. 2010. The evolution of thrombospondins and their ligand-
889 binding activities. *Molecular Biology and Evolution*, 27, 2187-2197.

- 890 BOSCH, T. C. G. & MCFALL-NGAI, M. J. 2011. Metaorganisms as the new frontier. *Zoology*,
891 114, 185-190.
- 892 BURKI, F., SHALCHIAN-TABRIZI, K. & PAWLOWSKI, J. 2008. Phylogenomics reveals a
893 new ‘megagroup’ including most photosynthetic eukaryotes. *Biology Letters*, 4, 366-369.
- 894 CALDERÓN, J. C., CURTIDOR, H., GONZÁLEZ, O., CIFUENTES, G., REYES, C. &
895 PATARROYO, M. E. 2008. High affinity interactions between red blood cell receptors
896 and synthetic *Plasmodium* thrombospondin-related apical merozoite protein (PTRAMP)
897 peptides. *Biochimie*, 90, 802-810.
- 898 DAVIS, A. K., MAKAR, R. S., STOWELL, C. P., KUTER, D. J. & DZIK, W. H. 2009.
899 ADAMTS13 binds to CD36: a potential mechanism for platelet and endothelial
900 localization of ADAMTS13. *Transfusion*, 49, 206-213.
- 901 DAVY, S. K., ALLEMAND, D. & WEIS, V. M. 2012. Cell biology of cnidarian-dinoflagellate
902 symbiosis. *Microbiology and Molecular Biology Reviews*, 76, 229-261.
- 903 DEL VALLE CANO, M., KARAGIANNIS, E. D., SOLIMAN, M., BAKIR, B., ZHUANG, W.,
904 POPEL, A. S. & GEHLBACH, P. L. 2009. A Peptide Derived from Type 1
905 Thrombospondin Repeat-Containing Protein WISP-1 Inhibits Corneal and Choroidal
906 Neovascularization. *Investigative ophthalmology & visual science*, 50, 3840-3845.
- 907 DETOURNAY, O., SCHNITZLER, C. E., POOLE, A. & WEIS, V. M. 2012. Regulation of
908 cnidarian-dinoflagellate mutualisms: Evidence that activation of a host TGF β innate
909 immune pathway promotes tolerance of the symbiont. *Developmental and Comparative
910 Immunology*, 38, 525-537.
- 911 DUNN, S. R., PHILLIPS, W. S., GREEN, D. R. & WEIS, V. M. 2007. Knockdown of actin and
912 caspase gene expression by RNA interference in the symbiotic anemone *Aiptasia pallida*.
913 *The Biological Bulletin*, 212, 250-258.
- 914 EBERL, G. 2010. A new vision of immunity: homeostasis of the superorganism. *Mucosal
915 Immunol*, 3, 450-460.
- 916 FERNANDO, T., FLIBOTTE, S., XIONG, S., YIN, J., YZEIRAJ, E., MOERMAN, D. G.,
917 MELENDEZ, A. & SAVAGE-DUNN, C. 2011. *C. elegans* ADAMTS ADT-2 regulates
918 body size by modulating TGF β signaling and cuticle collagen organization.
919 *Developmental biology*, 352, 92-103.
- 920 GOLDSTEIN, B. & KING, N. 2016. The Future of Cell Biology: Emerging Model Organisms.
921 *Trends in Cell Biology*, 26, 818-824.
- 922 GRABHERR, M. G., HAAS, B. J., YASSOUR, M., LEVIN, J. Z., THOMPSON, D. A., AMIT,
923 I., ADICONIS, X., FAN, L., RAYCHOWDHURY, R., ZENG, Q., CHEN, Z.,
924 MAUCELI, E., HACOHEN, N., GNIRKE, A., RHIND, N., DI PALMA, F., BIRREN, B.
925 W., NUSBAUM, C., LINDBLAD-TOH, K., FRIEDMAN, N. & REGEV, A. 2011. Full-

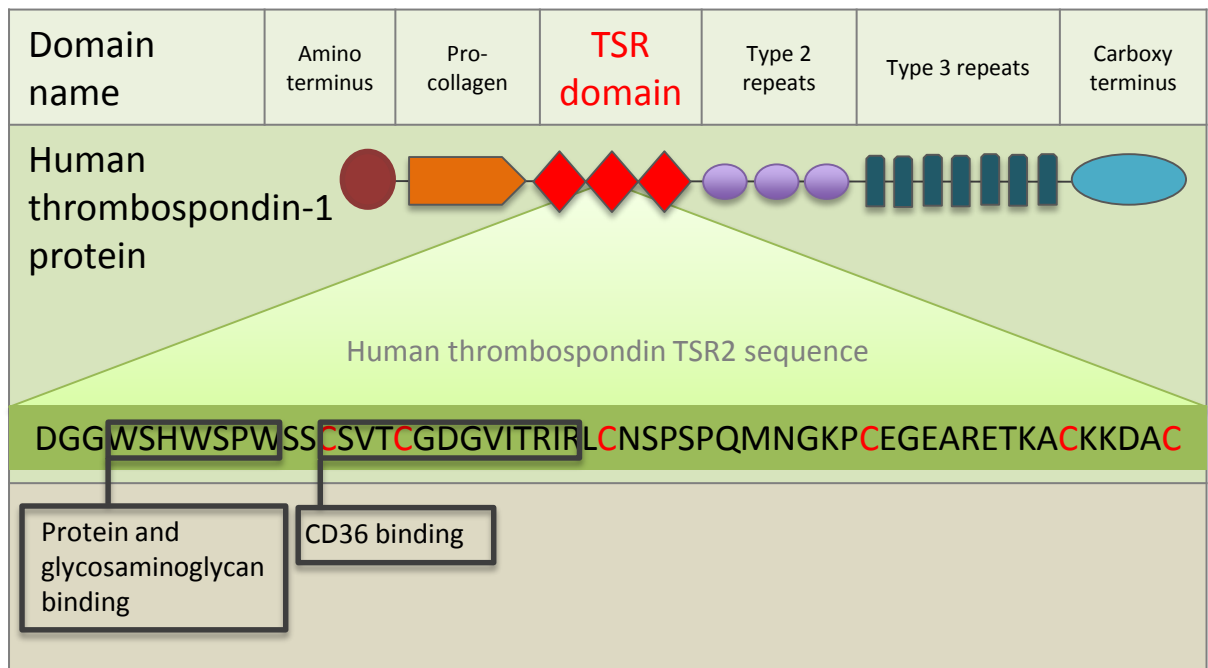
- length transcriptome assembly from RNA-Seq data without a reference genome. *Nature Biotechnology*, 29, 644-652.
- HAMADA, M., SHOGUCHI, E., SHINZATO, C., KAWASHIMA, T., MILLER, D. J. & SATOH, N. 2013. The complex NOD-like receptor repertoire of the coral *Acropora digitifera* Includes novel domain combinations. *Molecular Biology and Evolution*, 30, 167-176.
- HAMAGUCHI-HAMADA, K., KURUMATA-SHIGETO, M., MINOBE, S., FUKUOKA, N., SATO, M., MATSUFUJI, M., KOIZUMI, O. & HAMADA, S. 2016. Thrombospondin Type-1 Repeat Domain-Containing Proteins Are Strongly Expressed in the Head Region of *Hydra*. *PloS one*, 11, e0151823.
- HOURCADE, D. E. 2006. The role of properdin in the assembly of the alternative pathway C3 convertases of complement. *Journal of Biological Chemistry*, 281, 2128-2132.
- KAPPE, S., BRUDERER, T., GANTT, S., FUJIOKA, H., NUSSENZWEIG, V. & MENARD, R. 1999. Conservation of a gliding motility and cell invasion machinery in apicomplexan parasites. *J Cell Biol*, 147, 937-944.
- KARAGIANNIS, E. D. & POPEL, A. S. 2007. Peptides derived from type I thrombospondin repeat-containing proteins of the CCN family inhibit proliferation and migration of endothelial cells. *The international journal of biochemistry & cell biology*, 39, 2314-2323.
- KEARSE, M., MOIR, R., WILSON, A., STONES-HAVAS, S., CHEUNG, M., STURROCK, S., BUXTON, S., COOPER, A., MARKOWITZ, S., DURAN, C., THIERER, T., ASHTON, B., MEINTJES, P. & DRUMMOND, A. 2012. Geneious Basic: an integrated and extendable desktop software platform for the organization and analysis of sequence data. *Bioinformatics*, 28, 1647-1649.
- KHALIL, N. 1999. TGF- β : from latent to active. *Microbes and Infection*, 1, 1255-1263.
- KITCHEN, S. A., CROWDER, C. M., POOLE, A. Z., WEIS, V. M. & MEYER, E. 2015. De novo assembly and characterization of four anthozoan (phylum Cnidaria) transcriptomes. *G3: Genes/ Genomes/ Genetics*, 5, 2441-2452.
- KOLI, K., SAHARINEN, J., HYYTIAINEN, M., PENTTINEN, C. & KESKI-OJA, J. 2001. Latency, activation, and binding proteins of TGF- β . *Microscopy research and technique*, 52, 354-362.
- KVENNEFORS, E. C. E., LEGGAT, W., HOEGH-GULDBERG, O., DEGNAN, B. M. & BARNES, A. C. 2008. An ancient and variable mannose-binding lectin from the coral *Acropora millepora* binds both pathogens and symbionts. *Developmental & Comparative Immunology*, 32, 1582-1592.
- KVENNEFORS, E. C. E., LEGGAT, W., KERR, C. C., AINSWORTH, T. D., HOEGH-GULDBERG, O. & BARNES, A. C. 2010. Analysis of evolutionarily conserved innate

- 963 immune components in coral links immunity and symbiosis. *Developmental and*
964 *Comparative Immunology*, 34, 1219-1229.
- 965 LANGE, C., HEMMRICH, G., KLOSTERMEIER, U. C., LÓPEZ-QUINTERO, J. A., MILLER,
966 D. J., RAHN, T., WEISS, Y., BOSCH, T. C. G. & ROSENSTIEL, P. 2011. Defining the
967 origins of the NOD-like receptor system at the base of animal evolution. *Molecular*
968 *Biology and Evolution*, 28, 1687-1702.
- 969 LEHNERT, E. M., BURRIESCI, M. S. & PRINGLE, J. R. 2012. Developing the anemone
970 *Aiptasia* as a tractable model for cnidarian-dinoflagellate symbiosis: the transcriptome of
971 aposymbiotic *A. pallida*. *BMC genomics*, 13, 271.
- 972 LEHNERT, E. M., MOUCHKA, M. E., BURRIESCI, M. S., GALLO, N. D., SCHWARZ, J. A.
973 & PRINGLE, J. R. 2014. Extensive differences in gene expression between symbiotic
974 and aposymbiotic Cnidarians. *G3: Genes/Genomes/Genetics*, 4, 277-295.
- 975 LI, W., HOWARD, R. & LEUNG, L. 1993. Identification of SVTCG in thrombospondin as the
976 conformation-dependent, high affinity binding site for its receptor, CD36. *Journal of*
977 *Biological Chemistry*, 268, 16179-16184.
- 978 LI, X. & LEE, A. Y. W. 2010. Semaphorin 5A and plexin-B3 inhibit human glioma cell motility
979 through RhoGDI α -mediated inactivation of Rac1 GTPase. *Journal of Biological*
980 *Chemistry*, 285, 32436-32445.
- 981 LIEW, Y. J., ARANDA, M. & VOOLSTRA, C. R. 2016. Reefgenomics. Org-a repository for
982 marine genomics data. *Database*, 2016, baw152.
- 983 MASLI, S., TURPIE, B. & STREILEIN, J. W. 2006. Thrombospondin orchestrates the
984 tolerance-promoting properties of TGF β -treated antigen-presenting cells.
985 *International Immunology*, 18, 689-699.
- 986 MEYER, E. & WEIS, V. M. 2012. Study of cnidarian-algal symbiosis in the 'omics' age.
987 *Biological Bulletin*, 223, 44-65.
- 988 MOHAMED, A. R., CUMBO, V., HARI, S., SHINZATO, C., CHAN, C. X., RAGAN, M. A.,
989 BOURNE, D. G., WILLIS, B. L., BALL, E. E., SATOH, N. & MILLER, D. J. 2016. The
990 transcriptomic response of the coral *Acropora digitifera* to a competent *Symbiodinium*
991 strain: the symbiosome as an arrested early phagosome. *Molecular Ecology*, 25, 3127-
992 3141.
- 993 MORAHAN, B. J., WANG, L. & COPPEL, R. L. 2009. No TRAP, no invasion. *Trends in*
994 *Parasitology*, 25, 77-84.
- 995 MOYA, A., HUISMAN, L., BALL, E., HAYWARD, D., GRASSO, L., CHUA, C., WOO, H.,
996 GATTUSO, J. P., FORET, S. & MILLER, D. J. 2012. Whole transcriptome analysis of
997 the coral *Acropora millepora* reveals complex responses to CO₂-driven acidification
998 during the initiation of calcification. *Molecular ecology*, 21, 2440-2454.

- 999 MURPHY-ULLRICH, J. E. & POCZATEK, M. 2000. Activation of latent TGF- β by
1000 thrombospondin-1: mechanisms and physiology. *Cytokine & growth factor reviews*, 11,
1001 59-69.
- 1002 NEUBAUER, E. F., POOLE, A. Z., WEIS, V. M. & DAVY, S. K. 2016. The scavenger receptor
1003 repertoire in six cnidarian species and its putative role in cnidarian-dinoflagellate
1004 symbiosis. *PeerJ*, 4, e2692.
- 1005 PAN, G., LV, H., REN, H., WANG, Y., LIU, Y., JIANG, H. & WEN, J. 2010. Elevated
1006 expression of semaphorin 5A in human gastric cancer and its implication in
1007 carcinogenesis. *Life sciences*, 86, 139-144.
- 1008 PINHEIRO, J., BATES, D., DEBROY, S., SARKAR, D. & TEAM, R. C. 2016. nlme: Linear
1009 and nonlinear mixed effects models. R package version 3.1-128. *R Foundation for
1010 Statistical Computing, Vienna*.
- 1011 POOLE, A. Z., KITCHEN, S. A. & WEIS, V. M. 2016. The role of complement in cnidarian-
1012 dinoflagellate symbiosis and immune challenge in the sea anemone *Aiptasia pallida*.
1013 *Frontiers in microbiology*, 7.
- 1014 PUTNAM, N. H., SRIVASTAVA, M., HELLSTEN, U., DIRKS, B., CHAPMAN, J.,
1015 SALAMOV, A., TERRY, A., SHAPIRO, H., LINDQUIST, E., KAPITONOV, V. V.,
1016 JURKA, J., GENIKHOVICH, G., GRIGORIEV, I. V., LUCAS, S. M., STEELE, R. E.,
1017 FINNERTY, J. R., TECHNAU, U., MARTINDALE, M. Q. & ROKHSAR, D. S. 2007.
1018 Sea anemone genome reveals ancestral eumetazoan gene repertoire and genomic
1019 organization. *science*, 317, 86-94.
- 1020 R-CORE-TEAM 2012. R: A language and environment for statistical computing. R Foundation
1021 for Statistical Computing, Vienna, Austria. ISBN 3-900051-07-0, URL <http://www.R-project.org>.
- 1022
- 1023 RACHAMIM, T., MORGENSTERN, D., AHARONOVICH, D., BREKHMAN, V., LOTAN, T.
1024 & SHER, D. 2014. The dynamically-evolving nematocyst content of an Anthozoan, a
1025 Scyphozoan and a Hydrozoan. *Molecular biology and evolution*, msu335.
- 1026 RANGARAJU, S., KHOO, K. K., FENG, Z.-P., CROSSLEY, G., NUGENT, D., KHAYTIN, I.,
1027 CHI, V., PHAM, C., CALABRESI, P., PENNINGTON, M. W., NORTON, R. S. &
1028 CHANDY, K. G. 2010. Potassium channel modulation by a toxin domain in matrix
1029 metalloprotease 23. *Journal of biological chemistry*, 285, 9124-9136.
- 1030 RCORETEAM. 2015. *R: A language and environment for statistical computing* [Online].
1031 Vienna, Austria: R Foundation for Statistical Computing. Available: <http://www.R-project.org> [Accessed].
- 1032
- 1033 RODRIGUEZ-LANETTY, M., PHILLIPS, W. & WEIS, V. 2006. Transcriptome analysis of a
1034 cnidarian - dinoflagellate mutualism reveals complex modulation of host gene
1035 expression. *BMC Genomics*, 7, 23.

- 1036 SADANANDAM, A., ROSENBAUGH, E. G., SINGH, S., VARNEY, M. & SINGH, R. K.
1037 2010. Semaphorin 5A promotes angiogenesis by increasing endothelial cell proliferation,
1038 migration, and decreasing apoptosis. *Microvascular research*, 79, 1-9.
- 1039 SCHWARZ, J., BROKSTEIN, P., VOOLSTRA, C., TERRY, A., MILLER, D., SZMANT, A.,
1040 COFFROTH, M. & MEDINA, M. 2008. Coral life history and symbiosis: Functional
1041 genomic resources for two reef building Caribbean corals, *Acropora palmata* and
1042 *Montastraea faveolata*. *BMC Genomics*, 9, 97.
- 1043 SCHWARZ, R. S., HODES-VILLAMAR, L., FITZPATRICK, K. A., FAIN, M. G., HUGHES,
1044 A. L. & CADAVID, L. F. 2007. A gene family of putative immune recognition
1045 molecules in the hydroid *Hydractinia*. *Immunogenetics*, 59, 233-246.
- 1046 SHINZATO, C., SHOGUCHI, E., KAWASHIMA, T., HAMADA, M., HISATA, K., TANAKA,
1047 M., FUJIE, M., FUJIWARA, M., KOYANAGI, R., IKUTA, T., FUJIYAMA, A.,
1048 MILLER, D. J. & SATOH, N. 2011. Using the *Acropora digitifera* genome to understand
1049 coral responses to environmental change. *Nature*, 476, 320-323.
- 1050 SHOGUCHI, E., SHINZATO, C., KAWASHIMA, T., GYOJA, F., MUNGPAKDEE, S.,
1051 KOYANAGI, R., TAKEUCHI, T., HISATA, K., TANAKA, M., FUJIWARA, M.,
1052 HAMADA, M., SEIDI, A., FUJIE, M., USAMI, T., GOTO, H., YAMASAKI, S.,
1053 ARAKAKI, N., SUZUKI, Y., SUGANO, S., TOYODA, A., KUROKI, Y., FUJIYAMA,
1054 A., MEDINA, M., COFFROTH, M. A., BHATTACHARYA, D. & SATOH, N. 2013.
1055 Draft assembly of the *Symbiodinium minutum* nuclear genome reveals dinoflagellate gene
1056 structure. *Current Biology*, 23, 1399-1408.
- 1057 SILVERSTEIN, R. L. 2002. The face of TSR revealed: an extracellular signaling domain is
1058 exposed. *J Cell Biol*, 159, 203-206.
- 1059 SPITZER, D., MITCHELL, L. M., ATKINSON, J. P. & HOURCADE, D. E. 2007. Properdin
1060 can initiate complement activation by binding specific target surfaces and providing a
1061 platform for de novo convertase assembly. *The Journal of Immunology*, 179, 2600-2608.
- 1062 SUGIMOTO, M., FUJIKAWA, A., WOMACK, J. E. & SUGIMOTO, Y. 2006. Evidence that
1063 bovine forebrain embryonic zinc finger-like gene influences immune response associated
1064 with mastitis resistance. *Proceedings of the National Academy of Sciences*, 103, 6454-
1065 6459.
- 1066 TAN, K., DUQUETTE, M., LIU, J., DONG, Y., ZHANG, R., JOACHIMIAK, A., LAWLER, J.
1067 & WANG, J. 2002. Crystal structure of the TSP-1 type 1 repeats: a novel layered fold
1068 and its biological implication. *Journal of Cell Biology*, 159, 373-382.
- 1069 TOLSMA, S. S., VOLPERT, O. V., GOOD, D. J., FRAZIER, W. A., POLVERINI, P. J. &
1070 BOUCK, N. 1993. Peptides derived from two separate domains of the matrix protein
1071 thrombospondin-1 have anti-angiogenic activity. *The Journal of cell biology*, 122, 497-
1072 511.

- 1073 TUCKER, R. P. 2004. The thrombospondin type 1 repeat superfamily. *The International Journal*
1074 *of Biochemistry & Cell Biology*, 36, 969-974.
- 1075 TUCKER, R. P., HESS, J. F., GONG, Q., GARVEY, K., SHIBATA, B. & ADAMS, J. C. 2012.
1076 A thrombospondin in the anthozoan *Nematostella vectensis* is associated with the nervous
1077 system and upregulated during regeneration. *Biology Open*.
- 1078 VAUGHAN, A. M., ALY, A. S. I. & KAPPE, S. H. I. 2008. Malaria parasite pre-erythrocytic
1079 stage infection: gliding and hiding. *Cell Host & Microbe*, 4, 209-218.
- 1080 VOOLSTRA, C. R., LI, Y., LIEW, J., BAUMGARTEN, S., ZOCCOLA, D., FLOT, J.-F.,
1081 TAMBUETE, S., ALLEMAND, D. & ARANDA, M. In Review. Comparative analysis
1082 of the genomes of *Stylophora pistillata* and *Acropora digitifera* provides evidence for
1083 extensive differences between species of coral. *Scientific Reports*.
- 1084 WEIS, V. M., DAVY, S. K., HOEGH-GULDBERG, O., RODRIGUEZ-LANETTY, M. &
1085 PRINGLE, J. R. 2008. Cell biology in model systems as the key to understanding corals.
1086 *Trends in ecology & evolution*, 23, 369-376.
- 1087 WOLFOWICZ, I., BAUMGARTEN, S., VOSS, P. A., HAMBLETON, E. A., VOOLSTRA, C.
1088 R., HATTA, M. & GUSE, A. 2016. *Aiptasia sp.* larvae as a model to reveal mechanisms
1089 of symbiont selection in cnidarians. *Scientific Reports*, 6.
- 1090 YANG, Y. L., LIN, S. H., CHUANG, L. Y., GUH, J. Y., LIAO, T. N., LEE, T. C., CHANG, W.
1091 T., CHANG, F. R., HUNG, M. Y., CHIANG, T. A. & HUNG, C. Y. 2007. CD36 is a
1092 novel and potential anti-fibrogenic target in albumin-induced renal proximal tubule
1093 fibrosis. *Journal of Cellular Biochemistry*, 101, 735-44.
- 1094 ZHANG, X. & LAWLER, J. 2007. Thrombospondin-based antiangiogenic therapy.
1095 *Microvascular research*, 74, 90-99.
- 1096
- 1097



												Symbiotic species	
Protein name	Protein domain architecture	<i>Homo sapiens</i>	<i>Nematostella vectensis</i>	<i>Anthopleura elegantissima</i>	<i>Aiptasia</i> sp.	<i>Acropora digitifera</i>	<i>Acropora Milii</i>	<i>Stylophora pistillata</i>	<i>Fungia scutaria</i>				
Thrombospondins													
Thrombospondin1/2		2	0	0	0	0	0	0	0	0	0	0	0
3/4/5 and COMP		4	4	2	3	3	3	3	3	3	3	2	
ADAMTS Metalloproteases													
ADAMTS 1-19 Basic structure		5	0	1	0	1	0	3	0				
ADAMTS 9		2	0	0	0	1	0	0	0				
ADAMTS 6,7,10,12,16-19		8	0	0	1	0	1	1	1				
ADAMTS-like 1,2,3, and papilin		4	2	0	1	1	0	0	0				
Cnidarian ADAMTS-like	 	0	21	1	11	9	10	8	0				
		0	3	0	1	1	1	1	1				
Semaphorins													
SEMA 5A and B		2	1	1	1	1	1	1	1	0			
TSR domains only													
Properdin		1	0	0	0	0	0	0	0	0	0	0	0
Cnidarian TSR domain		0	50	7	22	6	2	14	6				
Astacin metallopeptidases													
Cnidarian astacin domain TSR proteins	 	0	1	2	4	0	0	1	0				
		0	1	3	10	0	0	4	0				
Trypsin													
Cnidarian trypsin domain TSR proteins		0	0	1	2	0	3	2	1				
VWA													
Cnidarian VWA domain TSR proteins		0	0	2	8	3	4	7	1				
		0	1	1	1	2	0	0	0				
Immunoglobulin containing TSR proteins													
Cnidarian immunoglobulin domain proteins	 	0	1	0	1	1	0	0	0				
		0	1	1	1	2	0	0	0				

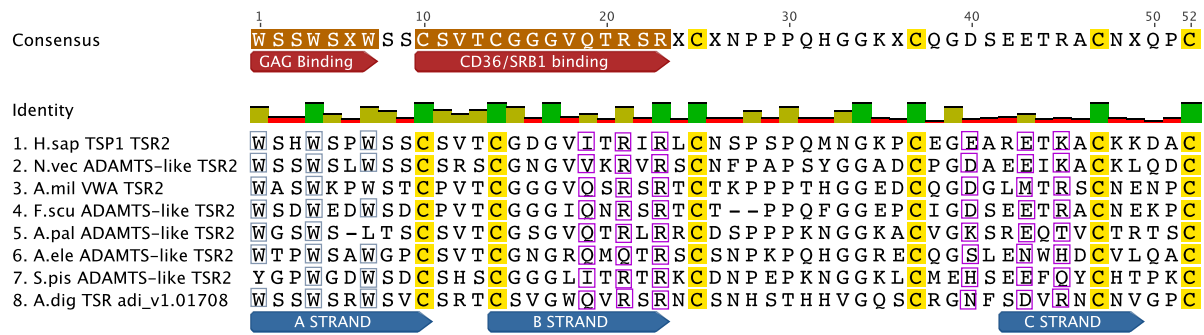


Figure 2 - figure supplement 1: The TSR domain is very well conserved from cnidarians up to humans, with binding motifs for glycosaminoglycans (GAGs) and the type B scavenger receptors, CD36/SRB1. All three-dimensional folding sites are present as described by Tan et al. (2002) for the crystal structure of human TSP1 TSR2. Six conserved cysteine residues are highlighted in yellow and form 3 disulfide bridges (C1-C5, C2-C6 and C3-C4). Three conserved tryptophan residues are shown in blue boxes and mark the 'WXXW' protein-binding motif. Amino acids that form the R layers are marked with purple boxes, and pairings forming 3 R layers are as follows: R3-R4, R2-R5 and R1-R6. The B strands are annotated at the bottom in blue strands A, B and C. Please refer to Tan et al. (2002) for a more detailed explanation of the three-dimensional folding.

Key			
	EGF domain		Transmembrane domain
	GPI anchor signal		TSR domain
	Signal peptide		Von Willebrand Factor A
Species	TRAP name	Domain organization	
<i>Symbiodinium minutum</i>	TSR ONLY	— — between 1-16 TSR repeats	
<i>Symbiodinium microadriaticum</i>	TSR ONLY	— — between 1-20 TSR repeats	
<i>Plasmodium falciparum</i>	TRAP CSP CTRP MTRAP	<p>Detailed description: This diagram shows four different domain organizations for Plasmodium falciparum. 1. TRAP: Starts with a brown circle (Signal peptide), followed by a blue arrow labeled 'VWA', then a red diamond (TSR domain), and ends with a purple wavy line (Transmembrane domain). 2. CSP: Starts with a brown circle, followed by a red diamond, then a blue square (GPI anchor signal), and ends with a purple wavy line. 3. CTRP: Starts with a brown circle, followed by a blue arrow labeled 'VWA', then two more blue arrows labeled 'VWA' (stacked), and ends with a purple wavy line. 4. MTRAP: Starts with a brown circle, followed by a red diamond, then another red diamond, and ends with a purple wavy line.</p>	
<i>Toxoplasma gondii</i>	TgMNP	<p>Detailed description: This diagram shows the domain organization for TgMNP. It starts with a brown circle (Signal peptide), followed by a blue arrow labeled 'VWA', then a red diamond (TSR domain), and ends with a purple wavy line (Transmembrane domain).</p>	
<i>Neospora caninum</i>	NcMNP	<p>Detailed description: This diagram shows the domain organization for NcMNP. It starts with a brown circle (Signal peptide), followed by a blue arrow labeled 'VWA', then a red diamond (TSR domain), and ends with a purple wavy line (Transmembrane domain).</p>	
<i>Eimeria tenella</i>	EtMIC1	<p>Detailed description: This diagram shows the domain organization for EtMIC1. It starts with a brown circle (Signal peptide), followed by a blue arrow labeled 'VWA', then a red diamond (TSR domain), and ends with a purple wavy line (Transmembrane domain).</p>	
<i>Eimeria maxima</i>	EmTFP250	<p>Detailed description: This diagram shows the domain organization for EmTFP250. It starts with a brown circle (Signal peptide), followed by a red diamond (TSR domain), then a purple oval labeled '(EGF X 31)', another purple oval, and a red diamond (TSR domain), and ends with a purple wavy line (Transmembrane domain).</p>	
<i>Babesia bovis</i>	BbTRAP	<p>Detailed description: This diagram shows the domain organization for BbTRAP. It starts with a brown circle (Signal peptide), followed by a blue arrow labeled 'VWA', then a red diamond (TSR domain), and ends with a purple wavy line (Transmembrane domain).</p>	
<i>Cryptosporidium</i> spp.	TRAP-C1	<p>Detailed description: This diagram shows the domain organization for TRAP-C1. It starts with a brown circle (Signal peptide), followed by a red diamond (TSR domain), and ends with a purple wavy line (Transmembrane domain).</p>	

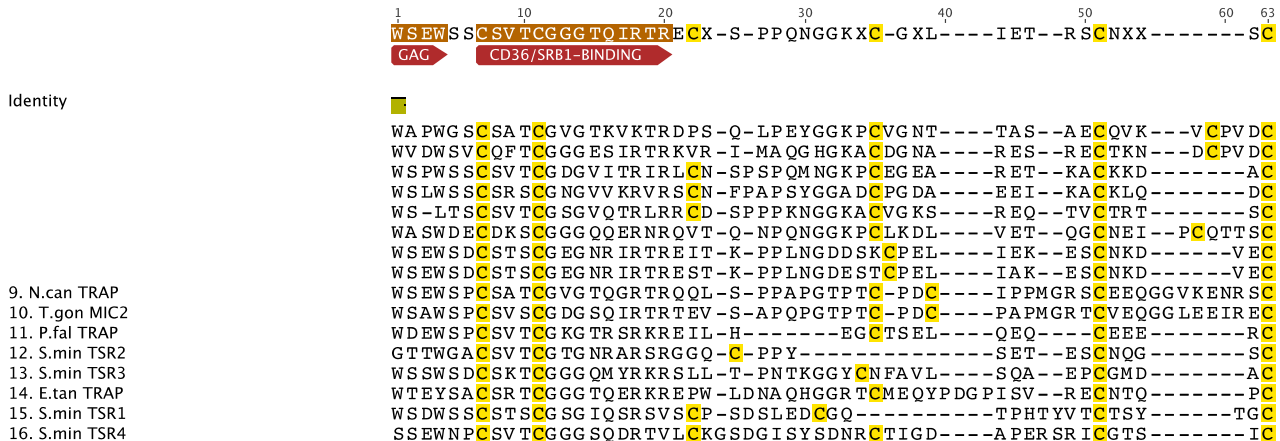
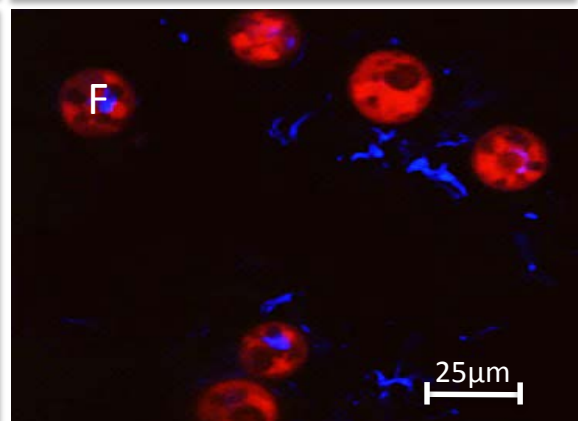
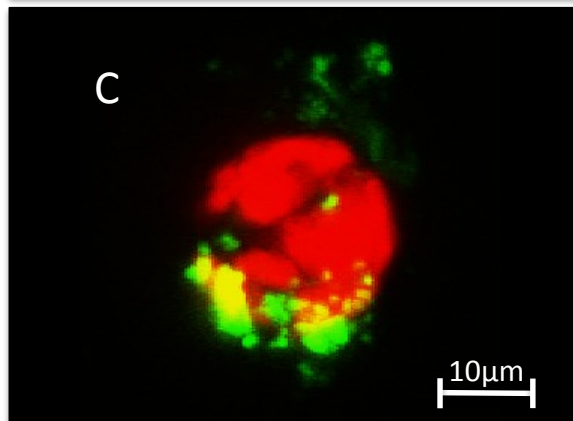
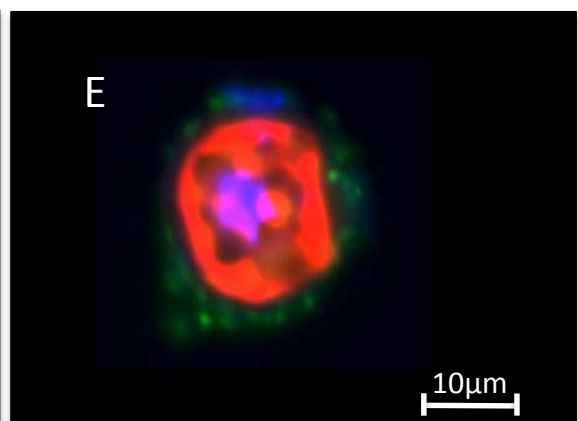
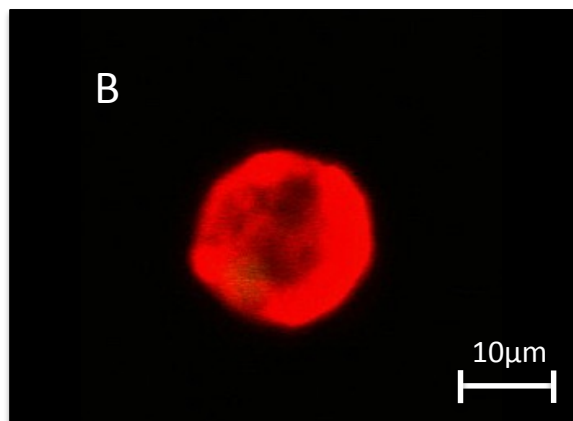
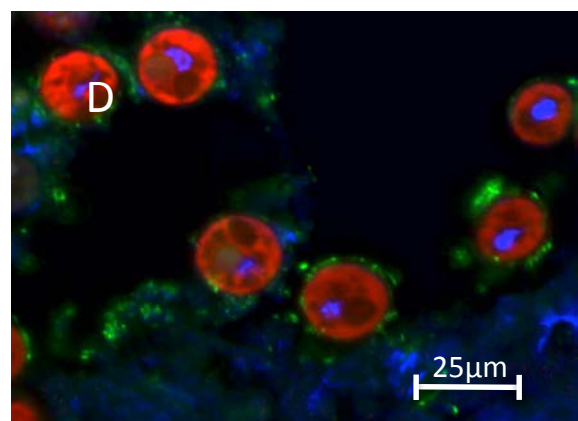
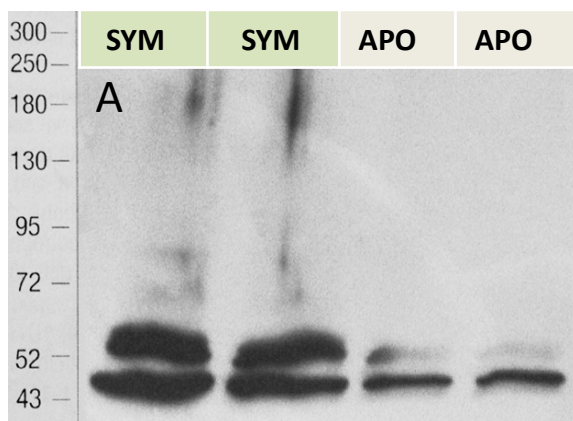


Figure 3 – figure supplement 1: TSR domain alignment compares apicomplexan TRAP TSR domains with TSR domains from the dinoflagellates *Symbiodinium minutum* and *S. microadriaticum*, TSR 2 from human TSP1, and ADAMTS-like TSR domains from the anemones *Nematostella vectensis* and *Aiptasia pallida*. Positioning and absence of specific cysteine residues (colored yellow) in TRAP and *Symbiodinium* TSRs will result in different patterns of disulfide bonds and three-dimensional folding. Binding sites for glycosaminoglycans (GAGs) and the scavenger receptors CD36/SRB1 (annotated in red) are somewhat conserved.



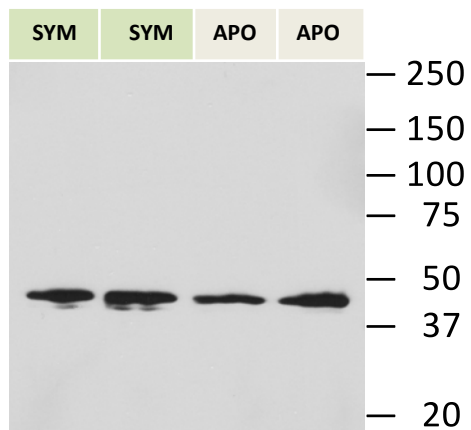


Figure 4 – figure
supplement 1. Actin
control for immunoblot
shown in Figure 4.

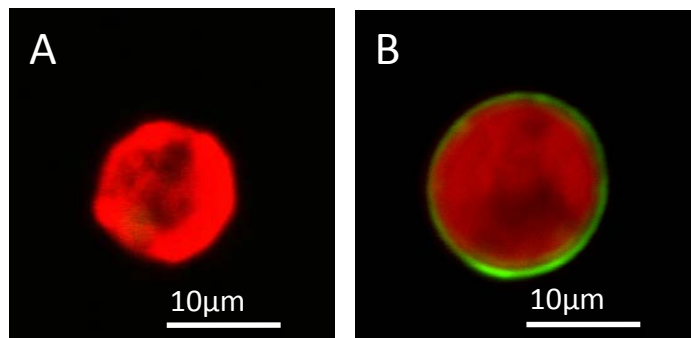
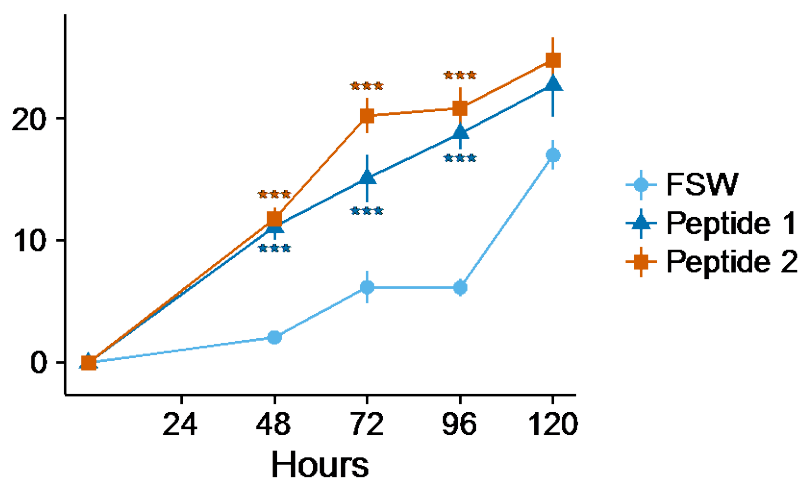
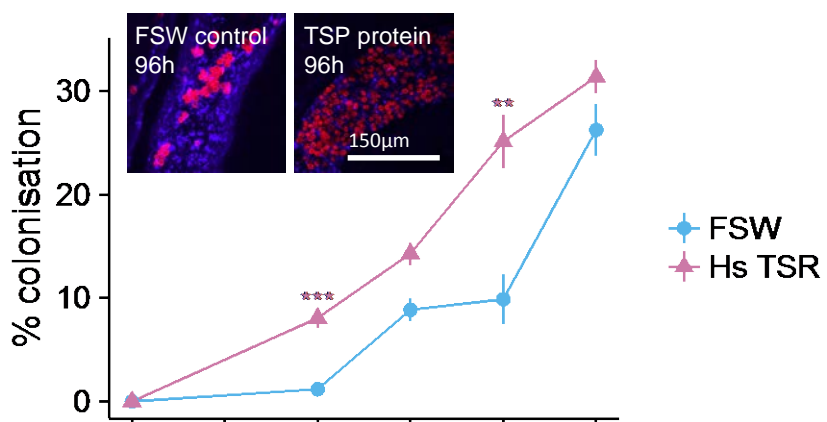
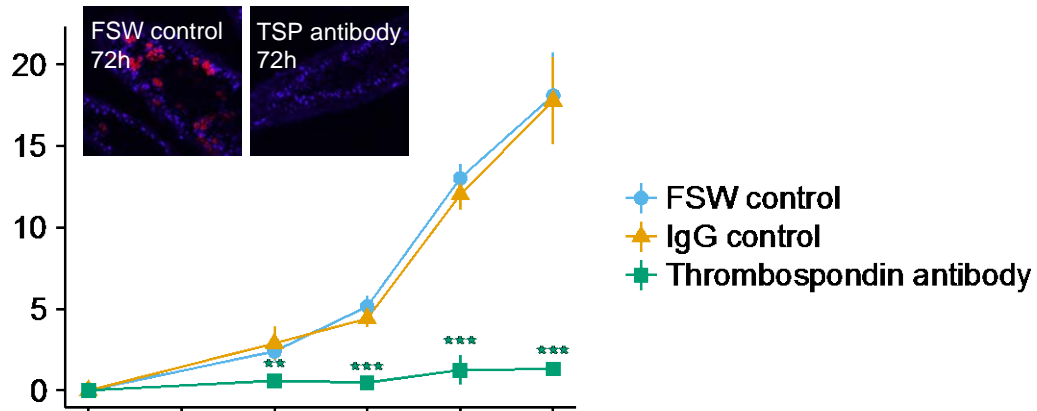
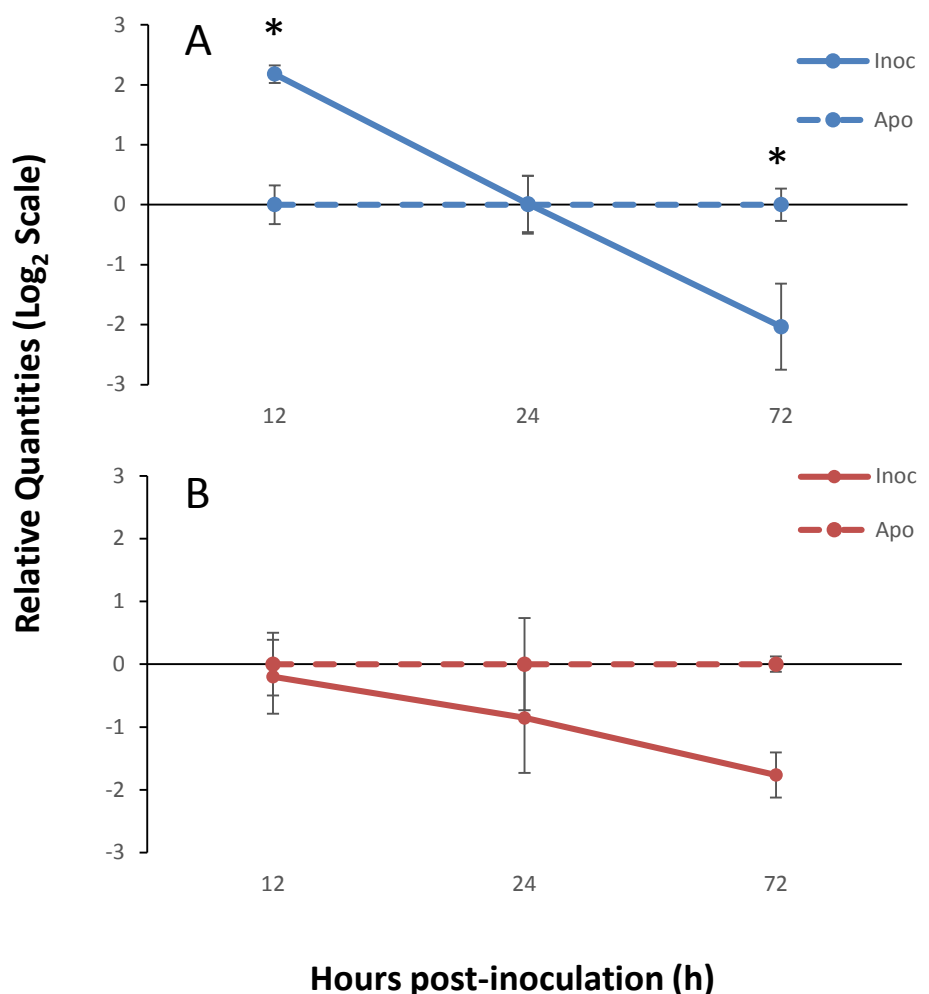


Figure 4 – figure supplement 2. Lipophilic membrane staining of dinoflagellate cells using Dil. Lipophilic membrane stain Dil was absent from (A) cultured algae but present in (B) freshly isolated symbionts. This is evidence of the presence of a symbiosome membrane surrounding freshly isolated symbionts.





Key



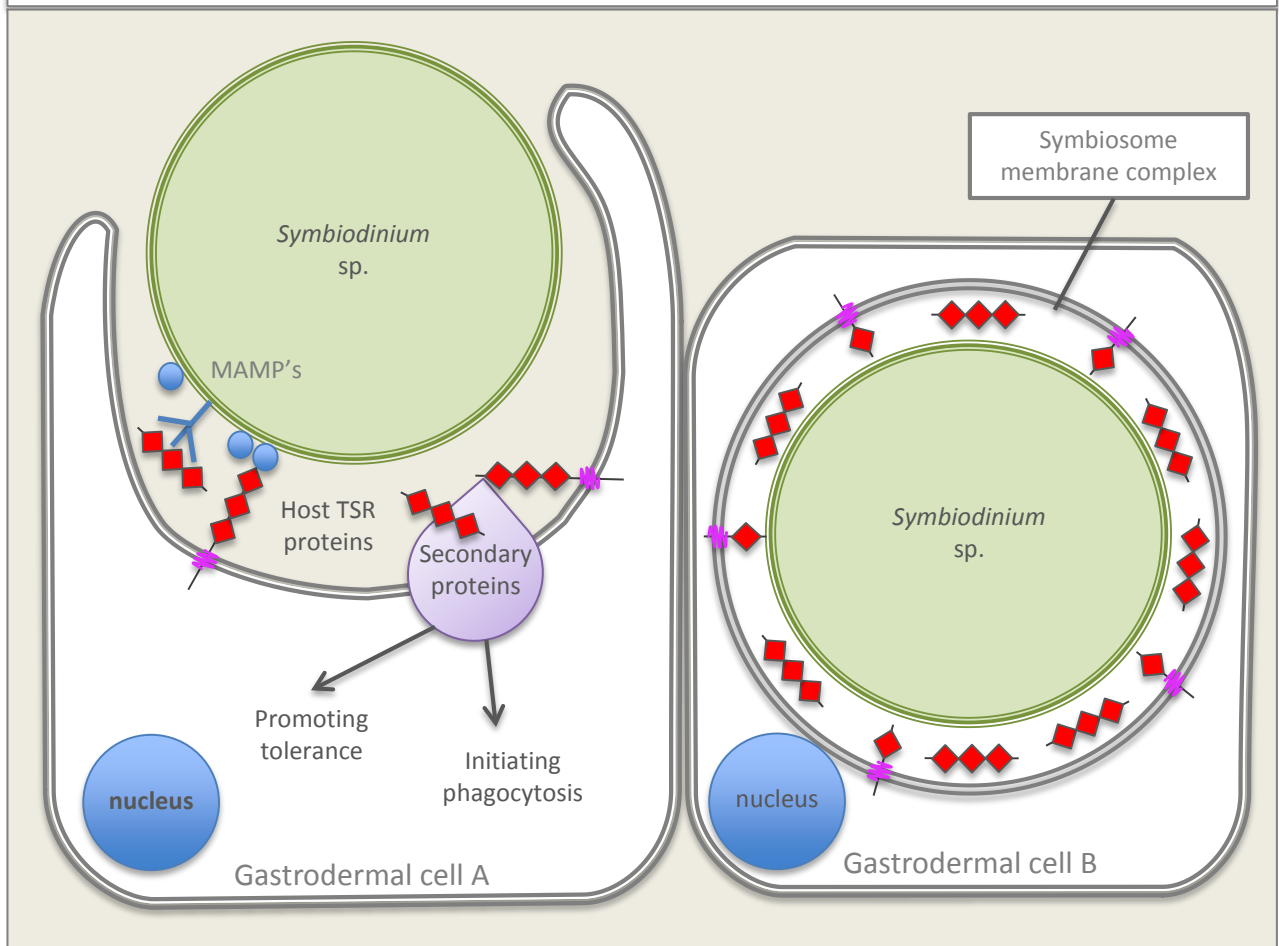
Microbe Associated Molecular Patterns (MAMP's)

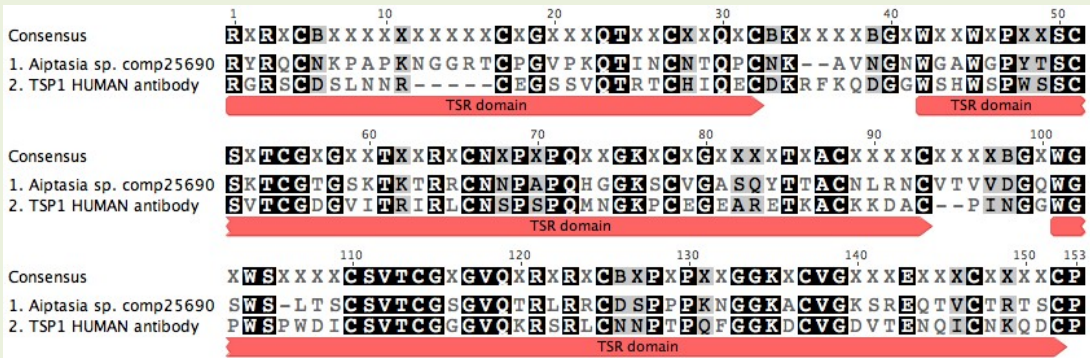
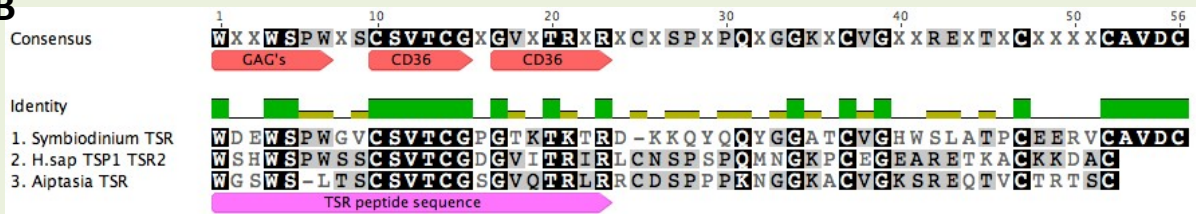


Transmembrane domain



TSR domain



A**B**

Aiptasia TSR peptide 1	WGWSLTCSVTCGSGVQTRLR	Molecular mass: 2371.7
Aiptasia TSR peptide 2	WGWSLTS ASVTAGSGVQTRLR	Molecular mass: 2307.57